

Complex Interfacial Behaviour of Mixtures of Fluorinated and Hydrogenated Alcohols

Miguel Cabrita Teixeira

Thesis to obtain the Master of Science Degree in

Materials Engineering

Supervisor: Doutor Eduardo Jorge Morilla Filipe

Co-Supervisor: Doutor Rogério Anacleto Cordeiro Colaço

Examination Committee

Chairperson: Doutor Luís Filipe da Silva dos Santos

Supervisor: Doutor Eduardo Jorge Morilla Filipe

Member of the committee: Doutor João Manuel da Costa e Araújo Pereira Coutinho

July of 2014

Agradecimentos

Em primeiro lugar gostaria de agradecer a oportunidade de ter trabalhado num laboratório de referência Mundial que me permitiu crescer academicamente e pessoalmente. Sem dúvida que o principal responsável por isso foi o Professor Doutor Eduardo Filipe que me convidou muito cedo para integrar este grupo. Todas as pessoas que passaram por este grupo foram essenciais para a minha evolução mas gostaria de agradecer especialmente ao Professor Doutor Eduardo Filipe e ao Doutor Pedro Morgado por toda a paciência e empenho com que abordaram todas as dúvidas e erros que fui cometendo ao longo destes últimos três anos e meio, sempre dispostos a impulsionar a minha aprendizagem. Sem dúvida que esta dissertação não seria possível sem eles e que o seu mérito e tempo despendido está presente ao longo das próximas páginas que eles com tanto rigor como vontade reviram. Também gostaria de fazer um especial agradecimento ao Pedro Duarte por ter ajudado a discutir todos estes temas e desenvolvido um programa que aumentou ainda mais o conhecimento que se pôde retirar de toda esta jornada de investigação.

Ao Professor Doutor José Nuno Canongia Lopes, que me proporcionou durante estes últimos seis meses uma bolsa de investigação para desenvolver uma investigação sobre propriedades de superfície de líquidos iónicos.

Ao Professor Doutor Rogério Colaço por ser co-orientador e ter proporcionado a tecnologia e conhecimento para o trabalho desenvolvido em AFM, que se tornou central nesta dissertação. Um especial agradecimento à Professora Doutor Patrícia Almeida e ao Pedro Nolasco por também terem partilhado os seus conhecimentos sobre a técnica de AFM.

A todos os professores, uns mais exigentes que outros, por tudo o que me foram ensinando durante estes últimos cinco anos.

Durante este percurso no Técnico vários foram os momentos que apenas foram superados com sucesso devido aos meus colegas que se foram tornando grandes amigos. Obviamente que estes cinco anos nunca serão esquecidos e toda a partilha e conhecimento que adquiri da experiência académica, profissional e pessoal de todos eles contribuíram para hoje ser quem sou.

Por fim, apesar de a influência não ter sido direta nas matérias aprendidas ao longo do curso, gostaria de agradecer à minha Família e à minha noiva por terem criado as bases e terem partilhado momentos comigo que me permitiram ter ultrapassado estes cinco anos da melhor maneira possível.

Resumo

Neste trabalho foi estudado o comportamento interfacial de misturas de álcoois fluorados e hidrogenados.

Foram medidas as tensões superficiais de 2,2,2-Trifluoroetanol (TFE) e das suas misturas com etanol, 1-propanol, 1-butanol e tert-butanol. Em todas as misturas foi observada aneotropia. Também foram medidos os volumes de excesso das misturas que são positivos, aumentando com o tamanho da cadeia do álcool hidrogenado. As misturas demonstram um comportamento complexo que indica uma elevada coesão no seio do líquido e fracas forças coesivas à superfície.

Foram também preparados filmes de Langmuir de 1H,1H-Perfluoro-1-tetradecanol (14F), 1H,1H,-Perfluoro-1-octadecanol (18F) e 1-Octadecanol (18H) e suas misturas, transferidos para a superfície de wafers de silício, e analisados por AFM. Os filmes de 18F formam espontaneamente domínios hexagonais a densidades superficiais baixas. Os domínios são compatíveis com cristais 2D que fundem a temperaturas mais elevadas, formando domínio circulares. Os filmes de 14F à temperatura ambiente formam uma estrutura rendilhada, parecendo cristalizar a mais baixa temperatura. As misturas de 14F e 18F formam domínios com características dos filmes de ambos os álcoois puros. As simulações de dinâmica molecular parecem confirmar a maior tendência das espécies fluoradas para cristalizar à superfície de água, enquanto as espécies hidrogenadas tendem a formar domínios líquidos.

Os filmes de Langmuir-Blodgett das misturas de 18H e 18F apresentam domínios circulares e hexagonais sugerindo a ocorrência de separação de fases 2D, apesar das simulações não mostrarem evidências de separação de fases naquela escala temporal.

Palavras-Chave: Filmes de Langmuir; Álcoois fluorados; AFM; Tensão superficial, Aneotropia

Abstract

The interfacial behaviour of mixtures of fluorinated and hydrogenated alcohols was studied.

The surface tension of pure trifluoroethanol (TFE) and of mixtures of TFE with ethanol, 1-propanol, 1-butanol and tert-butanol was measured. All mixtures display minima. The excess molar volumes of the mixtures were also measured and found to be positive, increasing with the chain length of hydrogenated alcohol. The mixtures display a complex behaviour that indicate high cohesion in the bulk and low cohesive forces at the interface.

Langmuir films of 1H,1H-Perfluoro-1-tetradecanol (14F), 1H,1H,-Perfluoro-1-octadecanol (18F) and 1-Octadecanol (18H) and their mixtures were prepared, transferred to the surface of silicon wafers and analysed by AFM. Films of pure 18F display starry-hexagonal domains that form spontaneously at room temperature and low surface density. The domains are compatible with 2D crystals and seem to melt at higher temperature forming circular domains. Films of pure 14F at room temperature display a “lacy” pattern that seem to crystalize at low temperature. Mixtures of 14F and 18F display a combination of the “lacy” patterns and hexagonal domains characteristic of the pure alcohols. Molecular dynamics simulations of the pure Langmuir films seem to confirm the tendency of fluorinated species to crystalize at the surface of water, while hydrogenated species form liquid-like domains.

Langmuir-Blodgett films of a mixture of 18H and 18F display circular and hexagonal domains suggesting that the two alcohols phase separate in 2D. Simulations showed no evidence of phase separation within the time scale of the simulation.

Key words: Langmuir films; Fluorinated alcohols; AFM; Surface tension; aneotropy

Index

Agradecimientos.....	II
Resumo	III
Abstract	IV
Index.....	V
Figures.....	VII
Tables.....	IX
1. Introduction	1
1.1. Motivation and objectives	1
1.2. Fluorinated and Hydrogenated Alcohols	1
1.3. Surface Tension.....	5
1.4. Langmuir Balance, Langmuir-Blodgett films and AFM.....	6
1.5. Molecular Dynamics Simulations.....	10
2. Experimental.....	11
2.1. Materials	11
2.2. Surface Tension.....	12
2.3. Excess molar volumes.....	13
2.4. Monolayers and AFM	13
2.5. Molecular Dynamics Simulations.....	15
3. Results and Discussion	17
3.1. Short chain Alcohols.....	17
3.1.1. Surface Tension of TFE as a function of Temperature	17
3.1.2. Surface Tension of mixtures of Hydrogenated and fluorinated alcohols.....	19
3.1.3. Excess molar volumes.....	21
3.1.4. Discussion	24
3.2. Long chain Alcohols	26
3.2.1. Langmuir and Langmuir-Blodgett films.....	26
3.2.2. Molecular Dynamics Simulations.....	38
3.2.3. Additional remarks	50
4. Conclusions	52
5. Future Work.....	53

6. Bibliography..... 54

Figures

Figure 1 - Representations of molecules studied in this work.....	3
Figure 2 – Cohesive forces in a liquid and at the surface.	5
Figure 3 – Generic Langmuir isotherm.....	7
Figure 4 – Monolayer evolution through air interface.....	7
Figure 5 - Hydrophilic Langmuir Blodgett method.....	8
Figure 6 - AFM scheme.....	9
Figure 7 - MD simulation simplified algorithm.	10
Figure 8 - Pendant drop apparatus example. ^[27]	12
Figure 9 – Initial configuration of 18H above water, 93Å ² /molecule.	15
Figure 10 - Surface Tension of TFE as a function of temperature.....	17
Figure 11 - Surface Tension of mixtures of hydrocarbon and fluorinated alcohols as a function of composition at 293.15K.....	20
Figure 12 - Redlich-Kister Regressions.	22
Figure 13 – Excess molar volume of hydrogenated alcohols and TFE mixtures. Points represent experimental results and the solid lines the Redlich-Kister equation.....	22
Figure 14 - Langmuir Isotherms of 18F and 18H, pure and mixtures, at 293.15K.....	26
Figure 15– AFM scan of mixture between 18F and 18H (0.8-0.2) at 70Å ² /molecule - topography contrast a), b) and c). d) and e) are height profiles.	28
Figure 16– AFM scan of a mixture between 18F and 18H (0.2-0.8) at 70Å ² /molecule. a) topography and b) phase contrast.....	29
Figure 17 - AFM scan of pure 18H at 20.3Å ² /molecule and 30mN/m - topography contrast.....	30
Figure 18 – AFM scan of pure 18F at 85Å ² /molecule - topography contrast.	31
Figure 19 - Langmuir balance Isotherm of 18F and 14F, pure and mixtures, at 293.15K.....	32
Figure 20 - AFM scan of pure 14F at 70Å ² /molecule – topography contrast.....	33
Figure 21 - AFM scan of mixture between 18F and 14F (0.8-0.2) at 80Å ² /molecule – topography contrast.....	34
Figure 22 - AFM scan of pure 18F at 30Å ² /molecule and 5mN/m and 308.15K – topography contrast.....	35
Figure 23 - AFM scan of pure 18F at 35Å ² /molecule and 5mN/m and 278.15K – topography contrast.....	36
Figure 24 - AFM scan of pure 14F at 32Å ² /molecule and 5mN/m 278.15K – phase contrast.....	36
Figure 25 - AFM scan of pure 18F by evaporation casting – phase contrast.	37
Figure 26 – a) 18H and b) 18F, above water after 25ps of simulation time.....	39
Figure 27 - Snapshots of 18H simulation during 5ns.	40
Figure 28 – Snapshots of 18F simulation during 5ns.....	41
Figure 29 – a) Lateral and b) vertical projections of 18F. Red spheres represent oxygen atoms of OH groups. Blue spheres represent the carbon atoms terminal CH ₃ groups.	42
Figure 30 - Snapshots of 14F simulation during 5ns.....	43

Figure 31 – a) Lateral and b) vertical projections of 14F. Red spheres represent oxygen atoms of OH groups. Blue spheres represent the carbon atoms terminal CH3 groups.	44
Figure 32 – Evolution of order parameter of Alcohols (18F, 14F, 18H) molecules in time.	44
Figure 33 – 14F immersion on water.	45
Figure 34 - Evolution of the order parameter of 18F at different temperatures in time, 278.15K, 293.15K, 308.15K.	46
Figure 35 - Evolution of the order parameter of 14F at different temperatures in time, 278.15K, 293.15K, 308.15K.	46
Figure 36 – a) Initial configuration of 18F + 14F mixture. b) Initial configuration of 18F + 18H mixture.	47
Figure 37 – a) Lateral and b) vertical projections of 18F-14F mixture, after 3ns. 18F are represented with terminal Carbon as Green and 14F with terminal Carbon as purple. The yellow line in Figure 37 b) represents the vertical plane observed in Figure 37b.	48
Figure 38 – a) Lateral and b) vertical projection of 18F-18H mixture, after 3ns. 18F are represented with terminal Carbon as Green and 18H with terminal Carbon as purple.	49
Figure 39 – Order Parameter as a function of time for both mixtures, 18F-14F and 18F-18H.	49
Figure 40 – Hexagonal Lattice.	51

Tables

Table 1 - Chemical compounds used in this work.....	11
Table 3 - Surface Tension of TFE as a function of temperature.	17
Table 4 - Surface Tension of mixtures of ethanol, butanol, propanol and tert-butanol with 2,2,2-Trifluoroethanol, at 293.15K.	19
Table 5 - Densities and excess molar volumes of mixtures of ethanol, butanol, propanol and tert-butanol with 2,2,2- Trifluoroethanol, at 293.15K and atmospheric pressure.....	21
Table 6 - Redlich-Kister adjustable coefficients for mixtures at 293.15K and atmospheric pressure.	22

1. Introduction

1.1. Motivation and objectives

Materials science has been pushing the limits of nanosciences through continually improving the control and accuracy of surface patterning. Surface patterning finds applications in a broad range of fields, from biology to the semiconductors industry. For example, silver nanoparticles are used in anti-microbial agents, patterns are used to functionalize surfaces making them hydrophobic or to increase the specific area of a catalyst, etc.

Organic thin films are attractive in such diverse fields because the properties of organic surfaces can be tuned by selectively modifying specific functional groups, while leaving the rest of the molecule unchanged. A good example is the gradual change of a hydrophobic to a hydrophilic surface by replacing CH₃ to OH groups. Self-assembled monolayers of organic substances find applications in several fields, from molecular membranes, surface patterning to self-lubricant surfaces.^[1]

Given its natural antipathy at the molecular level, mixtures of fluorinated and hydrogenated species are a very promising path to produce materials displaying surface patterning that can ultimately lead to selective adsorption.

The purpose of this thesis is to study the interfacial behaviour of mixtures of fluorinated and hydrogenated molecules and use their natural unfavourable interactions to obtain and control the formation of patterns.

1.2. Fluorinated and Hydrogenated Alcohols

Binary mixtures of alkanes and perfluoroalkanes are highly non-ideal in spite of the apparent similarity between these substances. They exhibit large regions of liquid–liquid immiscibility, large positive deviations from Raoult's law and large positive excess properties (such as the excess enthalpy and volume), a clear indication of weak unlike interactions. Since the late 40s the potential application of these systems as refrigerant mixtures or as immiscible solvents has motivated their study. However in recent years, perfluoroalkanes have become key fluids in a wide range of fields due to their chemical inertness, biocompatibility and peculiar physical properties^[2,3]. For example, from medical applications, where they find use as oxygen carriers in blood substitute formulations^[4] or as fluids in eye surgery, to technological applications as solvents for biphasic synthesis, fire-extinguishers or lubricants. As a result, considerable work has been done on the theoretical and computational modelling of n-alkane + n-perfluoroalkane mixtures^[5,6,7,8,9,10,11,12,13,14,15]. In particular, special attention has been given to understanding the unlike molecular interactions^[6,7,15]. These studies concluded that the usual Lorentz–Berthelot combining rules for the crossed intermolecular potential parameters fail to give satisfactory results, because of an unusually weak hydrocarbon–fluorocarbon attractive interaction.

Structurally, the substitution of hydrogens for the larger and heavier fluorine atoms results in a larger cross-sectional area for fluorinated chains (0.283 nm² compared to 0.185 nm²) and consequently higher

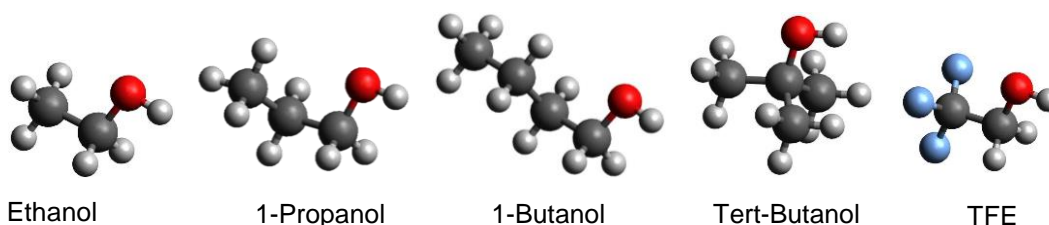
densities and molar volumes for n-perfluoroalkanes when compared with n-alkanes of the same number of carbon atoms.

Another important difference between fluorinated and hydrogenated chains is conformational. For the n-alkanes, the value of the dihedral angle at the energy minimum of a “trans” C-C bond is exactly 180°, so that the chains tend to be in their all-trans planar form. For the n-perfluoroalkanes, the dihedral angle at minimum energy is not exactly 180°, and as a consequence, perfluorinated chains display a helical conformation and rigidity, which contrasts with the flexible character of hydrogenated chains. It is believed that one of the consequences of chain stiffness in liquid fluorocarbons is less efficient molecular packing and the existence of “holes” in the liquid. This can explain (at least in part) the enhanced solubility of simple gases (e.g., oxygen, nitrogen, etc.) in liquid perfluoroalkanes.

The key idea of this project is to study the peculiar properties of mixtures of fluorinated and hydrogenated species at interfaces. In particular, the possibility of occurring phase separation at the interface will be investigated. Ultimately, the aim is to understand and control the resulting formation of domains/patterns.

Hydrogenated and fluorinated alcohols were chosen for this study. The presence of the OH group is useful to guarantee an adequate orientation and anchoring of the molecules at the interface. The possibility of strong interactions between the two types of alcohols through hydrogen bonding adds an extra interesting challenge to the investigation.

The interfacial behaviour of mixtures of hydrogenated and fluorinated alcohols, that simultaneously interact through strong hydrogen bonding, was thus inspected. In the case of short chain alcohols (trifluoroethanol, ethanol, 1-propanol, 1-butanol and tert-butanol) which are liquids at room temperature and soluble in water, surface tensions as a function of composition were measured as well as liquid densities. For long chain alcohols (1H,1H-Perfluoro-1-tetradecanol (14F), 1H,1H,-Perfluoro-1-octadecanol (18F) and 1-Octadecanol (18H)) which are solids and insoluble in water, Langmuir films at the surface of water were prepared, transferred to the surface of silicon wafers and analysed by atomic force microscopy (AFM). All films were studied by molecular dynamics computer simulation.



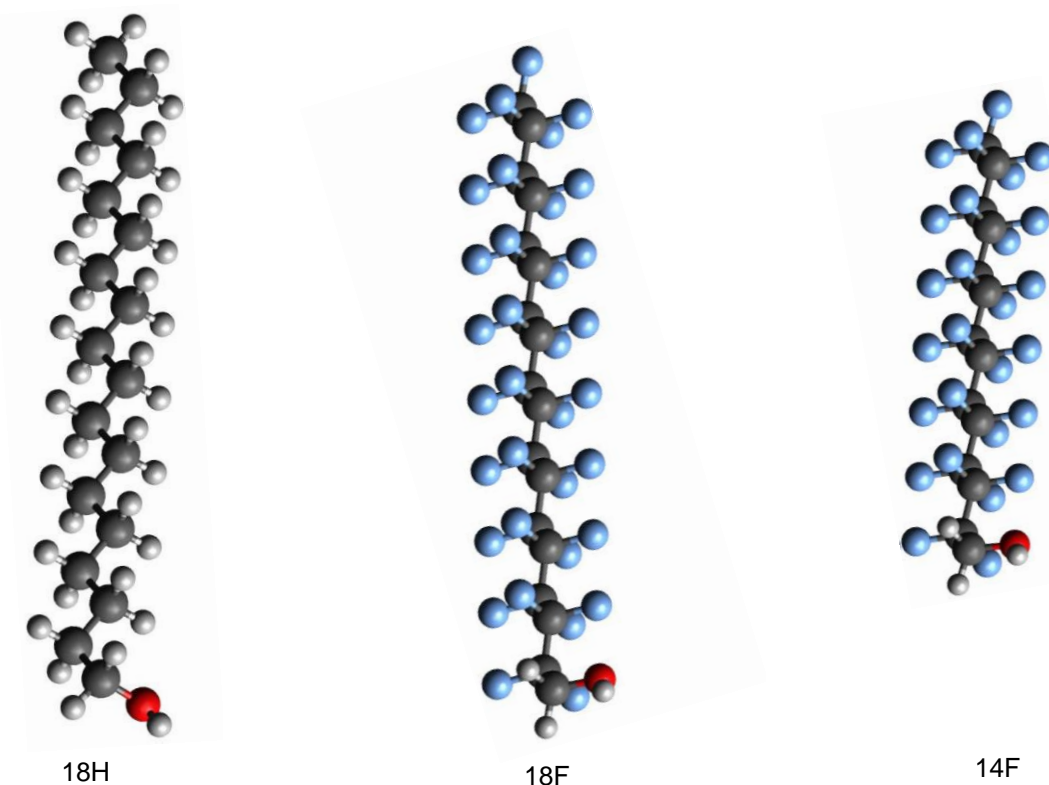


Figure 1 - Representations of molecules studied in this work.

Excess volumes for mixtures of TFE with short chain hydrogenated alcohols have been reported in the literature and in the case of TFE + ethanol, vapour-liquid equilibrium data and excess enthalpies are also found [16]. As for surface properties, no studies could be found in the literature.

Mixtures of TFE with short chain hydrogenated alcohols display a very complex behaviour when compared with mixtures of hydrogenated alcohols or with mixtures of alkanes and perfluoroalkanes: large and positive excess molar volumes are observed (unlike those of mixtures of hydrogenated alcohols with similar chain length, which are very small), as well as large and negative excess enthalpies (unlike those of mixtures of alkanes and perfluoroalkanes which are large and positive)^[5-15]. In a recent work [16] it was shown that the large negative excess enthalpy found for TFE + ethanol mixtures, result from a preferential hydrogen bond between the two alcohols. These mixtures thus have very complex bulk properties and it would be interesting to understand how they behave at the interface. Since there is a lack in literature of surface properties this work intends to fill this void.

Surface tensions of mixtures of alkanes and perfluoroalkanes have been described in the work of Mukerjee *et al.* [17] and Handa *et al.* [18] where a minimum in the surface tension of hexane and perfluorohexane mixture is reported. The minimum in the surface tension (aneotrope) of this mixture cannot be fully explained by simple models and is qualitatively interpreted as a consequence of weak cross interactions in the bulk.

Qaqish *et al.* [19] studied the phase separation of long chain fluorinated and hydrogenated acids at the air-water interface. No information could be found in the literature concerning mixtures of long chain

alcohols. In the work of Qaqish *et al.* domains are observed for mixtures of arachidic acid (C₁₉H₃₉COOH) and perfluorotetradecanoic acid (C₁₃F₂₇COOH). The observed structures are composed mainly of arachidic acid and the continuous phase is essentially the perfluorinated acid. Increasing temperature and time increase the size of the hexagonal domains. It was also found that shaking the spreading solutions prior to deposition may change the observed domains which is very intriguing. The mechanism proposed to explain the growth of the hexagonal domains is the 2D Ostwald ripening mechanism as an alternative to pure nucleation-and-growth mechanism ^[20].

1.3. Surface Tension

Surface tension ^[21] is a complex concept that can be analysed from different perspectives. Surface tension is the energy required to increase the surface area by unit of area or the force required to increase the surface by a unit of length. Traditionally surface tension is expressed in dyn/cm or erg/cm² but in SI units it is expressed in N/m or J/m².

Surface tension and cohesive forces are intimately connected and higher cohesive forces usually corresponds to higher surface tensions.

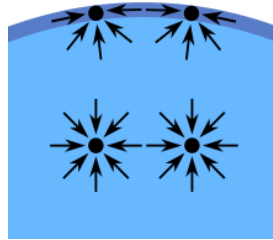


Figure 2 – Cohesive forces in a liquid and at the surface.

(http://en.wikipedia.org/wiki/Surface_tension, 2014/06/20)

Higher cohesive forces enhances the tendency of the surface to reduce its area in order to minimize its energy. From the energetic point of view, molecules at the surface are in a different condition from those in bulk. Contrarily to those in the bulk, surface molecules are not subjected to a uniform force field, since interactions with molecules in the vapour are weaker. Thus, the resulting net force at the surface attracts the molecules to the bulk. Energetics predicts that free energy of interface formation must be positive, otherwise the interface is unstable or metastable. In mixtures, it is common that molecules with lower surface tension migrate to the surface in order to minimize the overall energetic equilibrium ^[22]. The equilibrium for a typical surfactant is given by the Gibbs equation,

$$\partial\gamma = -\sum_1^n \Gamma_n \partial\mu_n \quad (1)$$

where $\partial\gamma$ is the change in the surface tension, Γ_n is the surface excess concentration of the n^{th} component and $\partial\mu_n$ is the change in the chemical potential of the n^{th} component.

$$\partial\mu_n = -RT \partial \ln a_n \quad (2)$$

$$\Gamma_n = \frac{n_i^{\text{total}} - n_i^{\text{liquid}} - n_i^{\text{vapor}}}{A} \quad (3)$$

where R is the gas constant, T is the absolute temperature, a_n is the activity of the n^{th} component in the bulk phase, n is the number of moles and A is the area. To calculate the excess surface concentration of dilute solutions, the surface tension of the mixture is represented as a function of concentration,

$$\Gamma_n = -\frac{1}{RT} \left(\frac{\partial\gamma}{\partial \ln C_n} \right) \quad (4)$$

where C_i is the concentration of the n^{th} component of the mixture.

1.4. Langmuir Balance, Langmuir-Blodgett films and AFM

A Langmuir trough was used to characterize and produce Langmuir-Blodgett films of long chain alcohols. [23, 24, 25]

Agnes Pockels, at the end of the 19th century, was a pioneer in the study of insoluble monomolecular films at the surface of water [26]. After her, Langmuir developed an intensive study about insoluble monolayers and started the study of what is commonly known as Langmuir films. Langmuir films are usually composed by molecules that are “anchored” at the surface of water by and hydrophilic part and the hydrophobic part extend through the air interface. Examples of these substances are alcohols, acids or phospholipids.

The area available, at the water surface, is controlled by a moving barrier that keeps insoluble molecules at only one side of the Langmuir Balance. As the film is being compressed different phases and equilibria occur at the surface of water. The film may exhibit different phases depending on temperature, subphase pH, ionic concentration of subphase and time dependent variables as rate of compression and annealing times.

The area available, at the water surface, is controlled by a moving barrier that keeps insoluble molecules at only one side of the Langmuir Balance. As the film is being compressed it can go through different phases and equilibria at the surface of water. The film may exhibit different phases depending on temperature, subphase pH, ionic concentration of subphase and time dependent variables as rate of compression and annealing times. Different phases are characterized by having different positional and orientational molecular arrangement. Hydrogenated alcohols are characterized by having at low pressure a liquid-vapour equilibrium, then a tilted condensed film and an untilted condensed monolayer (vertical molecules) [23].

The surface pressure defined as the difference between the surface tension of the subphase (γ_0) and the surface tension of the surface with the monolayer (γ) is recorded during compression..

$$\pi = \gamma_0 - \gamma \quad (5)$$

In Figure 3 a generic Langmuir isotherm is shown. This is a plot of the surface pressure vs area per molecule, a 2D analogue of the 3D pressure-volume diagrams. Different phases and types of phase equilibria can be inferred from the shape of Langmuir isotherm.

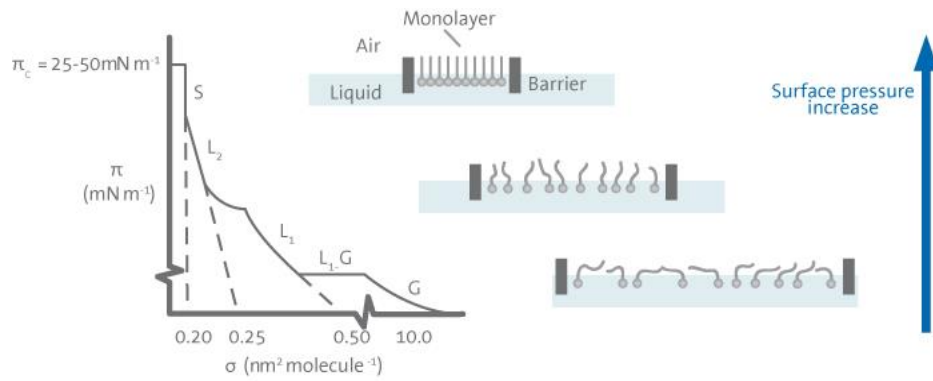


Figure 3 – Generic Langmuir isotherm.

<http://www.biolinscientific.com/technology/lb-ls-technique/>, 2014/06/23)

At high surface pressure different molecules behave differently. Some substances, due to the excess of lateral force, may collapse in the direction of air or in the direction of water and create vesicles. Other monolayers can even grow to trilayer or multilayer as illustrated in Figure 4.

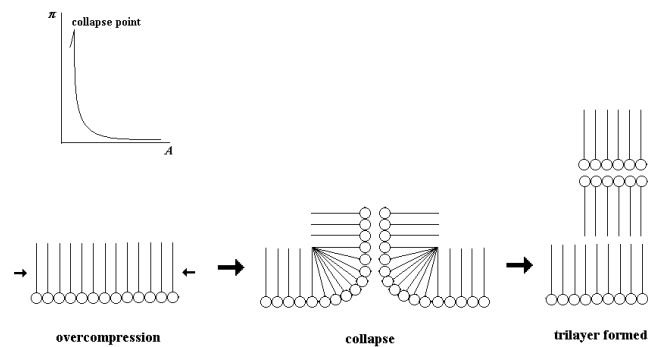


Figure 4 – Monolayer evolution through air interface.

<http://community.dur.ac.uk/sharon.cooper/lectures/colloids/interfacesweb2.html>, 2014/06/24)

The transfer of a Langmuir monolayer to the surface of a substrate is possible using the Langmuir-Blodgett technique (figure 5). In this process, the substrate must be immersed vertically in water before the spreading of the film. The film is then compressed until the desired surface pressure value, and the substrate is slowly raised. The now coated substrate may be dipped again, and a second layer will be transferred, 'back to back' with the first. Repeating the process allows the transfer of multilayers – even hundreds of layers. The surface pressure is kept constant during each transfer thanks to barrier mobility, thus assuring similar conditions for each layer transfer.

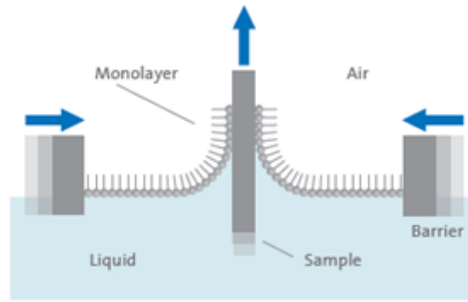


Figure 5 - Hydrophilic Langmuir Blodgett method.

<http://www.biolinscientific.com/technology/lb-ls-technique/>, 2014/07/30)

In order to characterize the films a number of experiments can be done, some *in loco*, such as Brewster Angle Microscopy (BAM), but other need the film to be previously extracted from the surface of water. Atomic Force Microscopy (AFM) cannot be done *in loco*, thus, Langmuir films must be transferred to a substrate, in this work the films were prepared by the Langmuir-Blodgett method.

Atomic force microscopy (AFM) was used to characterize the Langmuir-Blodgett films deposited on the silicon surface. AFM is a technique with nanometer-scale resolution in which a probe scans the surface of a sample recording changes in height, friction coefficient, etc. The probe consists on cantilever and a tip. A photo detector receives a laser light reflecting on the cantilever that measures the relative motion/position of the cantilever as can be seen in the representation in Figure 6.

There are several AFM techniques to scan the surface of samples. Due to the softness of the studied films, the scans were made using tapping mode. There are several types of contrast modes in the tapping mode. The topography contrast results from the differences in height in the sample. The phase contrast mode indicates the phase shift signal when compared to the free oscillating signal (soft materials will dissipate more energy increasing the signal delay, contrary to hard materials).

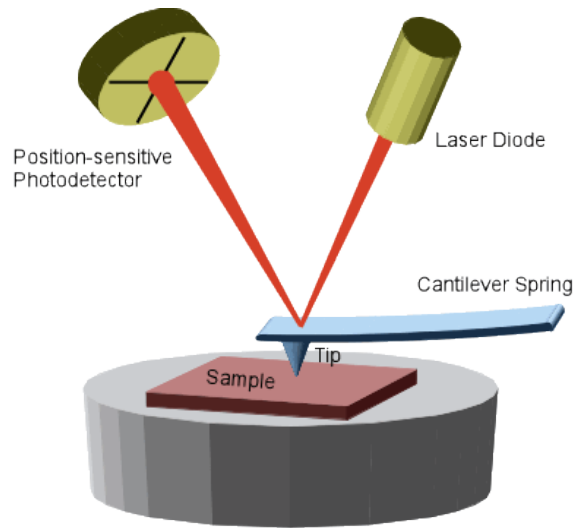


Figure 6 - AFM scheme.

<http://www3.physik.uni-greifswald.de/method/afm/eafm.htm>, 2014/06/20)

1.5. Molecular Dynamics Simulations

MD simulation were performed to obtain molecular level insight on the formation and structure of the Langmuir Films. MD simulations are a computational method in which Newton's equation of motion are solved, and the trajectory of particles calculated subjected to a specified force field.

MD has been used in different areas of knowledge, from biochemistry to material science or physics. MD is frequently used to refine structures of proteins or other macromolecules or to simulate lipid bilayers. Using MD it is now possible to study the molecular structure of a liquid or an interface in order to understand deeply the factors responsible for a specific behaviour. [27,28]

In order to implement a MD simulation an algorithm, such as the one shown in Figure 7 must be followed. In this work the *DL_POLY Classic* [29] software was used to perform the simulations.

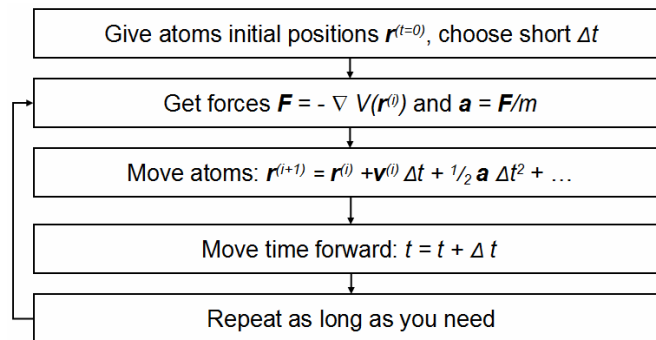


Figure 7 - MD simulation simplified algorithm.

2. Experimental

2.1. Materials

In Table 1 are listed the substances used in this work, their origin and reported purity.

Short chain hydrogenated alcohols were kept in molecular sieves with 0.3nm pores. Fluorinated alcohols were used as received. The water content of TFE was regularly checked using a Karl-Fischer coulometer. TFE was used under a dried nitrogen flux. It was found to decompose when kept in molecular sieves. All mixtures were prepared gravimetrically in an analytical balance (resolution of 1×10^{-5} g).

The solid alcohols were dissolved in a convenient spreading solvent. The fluorinated alcohols were dissolved in a mixture of 1,1,2-Trichlorotrifluoroethane (99.9+% Aldrich) and perfluorohexane (99% Aldrich) 9:1 (V:V). Hydrogenated alcohols were dissolved in Hexane (Merck). Concentrations on the order of 0.2 to 1 mg/mL were prepared, followed by at least 10min of ultrasonication. Perfluorohexane and hexane were kept in molecular sieves with 0.3nm pores. 1,1,2-trichlorotrifluoroethane was distilled and kept under nitrogen atmosphere. It was found to decompose when kept in molecular sieves.

The water used in cleaning or as the subphase was purified using Milli-Q system (Milipore). The solutions were spread with gas-tight Hamilton syringes (100 to 250 μ L).

Solid compounds were kept in a closed glass vessel in a dry atmosphere.

Table 1 - Chemical compounds used in this work.

Compound	Abbreviation	Formula	Purity	Company	Melting point (°C)
1-octadecanol	18H	CH ₃ (CH ₂) ₁₇ OH	99%	Sigma-Aldrich	56-59
1H,1H-Perfluoro-1-Octadecanol	18F	CF ₃ (CF ₂) ₁₆ CH ₂ OH	95%	Fluorochem, England	152-156
1H,1H-Perfluoro-1-Tetradecanol	14F	CF ₃ (CF ₂) ₁₂ CH ₂ OH	95%	Fluorochem, England	62-63
Ethanol	EtOH	CH ₃ CH ₂ OH	99.5%	Pancreac	-114
Propan-1-ol	PropOH	CH ₃ (CH ₂) ₂ OH	99.5%	Lab Scan	-126.15
1-Butanol	ButOH	CH ₃ (CH ₂) ₃ OH	99.8%	Sigma-Aldrich	-89
Tert-Butanol	Tert-ButOH	CH ₃ (CH ₂) ₃ OH	99.7%	Sigma-Aldrich	25
2,2,2-Trifluoroethan-1-ol	TFE	CF ₃ CH ₂ OH	99%	Apollo	-43.5

2.2. Surface Tension

The surface tension of short chain alcohols was measured by an optical tensiometer using the pendant drop method.

The surface tension of the liquid was measured by the pendant drop method. By taking a photograph of a suspended (assumed axisymmetric) drop, knowing the density of the liquid, the surface tension can be measured by approximating a solution of the Young-Laplace equation to the drop shape. This method is known as ADSA, axisymmetric drop shape analysis ^[30]. The software used in this work was developed by Neumann *et al.* ^[31].

The apparatus includes an aluminium temperature controlled chamber, a nitrogen inlet, the drop holder, an automated syringe and a glass cuvette. Firstly the chamber, the cuvette and the drop holder were cleaned using chloroform. After drying, the chamber is closed with the glass cuvette inside, the light and the thermostat are turned on and the chamber is continuously purged with a nitrogen flux. Some drops of the liquid are dropped in order to reach the equilibrium with its vapour. Only after temperature and movement stabilization, a drop is hanged in the drop holder and the photographs are acquired. Each experimental point is the average of at least 10 photographs of more than 10 different drops. Some liquids, due to evaporation, had to be continuously fed.

Controlling and measuring temperature was a challenging problem to overcome. Due to evaporation, the temperature of the drop tends to be different (lower) than the temperature of the chamber. Thus, a liquid buffer was built inside the chamber and a platinum thermometer was mounted at the tip of the drop holder. In this way it was possible to decrease the temperature change of the drops, thus measuring with higher accuracy and precision. All measurements were made at $293.15 \pm 0.1\text{K}$, unless said otherwise.

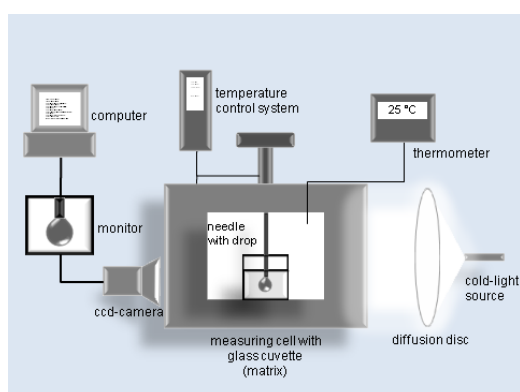


Figure 8 - Pendant drop apparatus example. ^[30]

2.3. Excess molar volumes

The densities were measured in a vibrating-tube Anton Paar DMA 5000 densimeter. The DMA 5000 has a built-in temperature control system, based on Peltier units, which is stable at $\pm 0.001\text{K}$. This densimeter was calibrated with water (distilled, deionized in a Milli-Q 185 Plus water purification system and freshly boiled) and at air at 20.000°C , taking into account atmospheric pressure. The calibration was checked with water over the whole range of operating temperatures, and the maximum deviation from literature values was found to be less than $2 \times 10^{-5} \text{ g cm}^{-3}$. The cleanliness of the measurement cell was verified at the beginning of each series of measurements by checking the measure of the density of air.

2.4. Monolayers and AFM

Langmuir films were produced on a NIMA trough type 601. A submerged platinum thermometer was used to register the temperature of the subphase. The surface tension was measured with a Wilhelmy plate sensor using a filter paper plate.

Initially the trough is cleaned with chloroform and rinsed several times with Millipore water, assuring no organic contaminants at the water surface. The desired quantity of the film-forming substance solution is spread drop by drop at the subphase surface with the help of a syringe. After waiting at least 10 minutes for solvent evaporation, the film can be compressed. The solutions are prepared before the deposition by weighting a certain amount of the long chain alcohol with a precision of $1 \times 10^{-5} \text{ g}$ in a calibrated flask of 25mL. The solutions of mixtures of alcohols are prepared by mixing solutions of pure compounds.

Langmuir-Blodgett films were prepared by placing a silicon wafer (8 cm^2) vertically in the water before the solution spread. Once the solution was spread and the solvent evaporated, the film was compressed up to the desired surface pressure / surface density. The deposition is made by carefully extracting the wafer from the water at a controlled speed and constant pressure. A hydrophilic substrate was needed to attach the alcohol groups to its surface. Silicon wafer was chosen due to its hydrophilic properties after proper treatment^[32]. The silicon wafers were scrubbed with an aqueous solution of detergent and rinsed with Millipore water. The wafer was then submersed in chromic mixture for at least 30 minutes and rinsed with Millipore water. The adhesion of the films to the surface of the silicon wafers were not investigated in detail. Throughout this work it is assumed that the film extraction process does not change the structure produced at the surface of water.

The compression speed ranged from 5 to 30 cm^2/min . Langmuir-Blodgett film were extracted at 3 mm/min . The temperature was kept constant at $\pm 1\text{K}$ during experiments.

Atomic force microscopy (AFM) was used to characterize the Langmuir-Blodgett films deposited on the silicon surface. Due to the softness of the studied films, the scans were made using tapping mode. Attempts made to scan the samples in contact mode proved to be unsuccessful. Images from 100 μm to 3 μm width were made with a NANOSENSOR PPP-NCLAuD tip (resonance frequency 204-497 kHz),

PID control parameters of P-2000, I-1000, D-0 and 256 lines per image and 256 points per line. Image treatments were performed using WSxM 5.0 software developed by Horcas *et al.*^[33] and consisted in Plane, Flatten, Equalize and line removal.

2.5. Molecular Dynamics Simulations

All simulations were performed using the *DL_POLY Classic* software. The raw data was analysed using the software integrated in *DL_POLY* package, as well as additional programs developed in our laboratory.

Alcohol molecules were modelled with the OPLS-AA force Field^[34]. Water was modelled with the three site spc-e rigid body model^[35]. Alcohol molecules were generated individually with the *AVOGADRO* software, their energy minimized and equilibrium conformations obtained. The coordinates of each molecule were then extracted, replicated to produce the required 2D grid and the simulation box assembled. These were then submitted to the *DL_POLY* software and simulation started.

All systems were simulated under NVT ensemble conditions using a Hoover thermostat and barostat with time constants of 0.5 and 2ps, respectively. Electrostatics interactions were treated using the Ewald summation method considering six reciprocal-space vectors, and repulsive-dispersive interactions were explicitly cut off at 1.6nm (long range corrections were applied assuming the system had a uniform density beyond this cut-off radius). All simulations were previously equilibrated with a *cut-off* of 1.2nm. This was done to decrease simulation time at first steps (~1.5ns). Each simulation contains 4000 water molecules and between 20 and 144 molecules of alcohols, add up between 14000 and 20000 site calculations.

Two simulation boxes of water and alcohol, were merged together a few Angstroms from each other. The water box was previously equilibrated in NPT conditions. The alcohol box was generated with alcohol molecules perpendicular to the water surface with the alcohol groups oriented towards water. Other attempts were made using previously equilibrated boxes of liquid alcohols but due to the low mobility of the molecules the evolution of the system is very slow, resulting in very long simulations. The simulations of the Langmuir films were performed in NVT conditions. The initial configuration of a typical Langmuir film simulation box containing 49 molecules of 18H is shown in Figure 9.

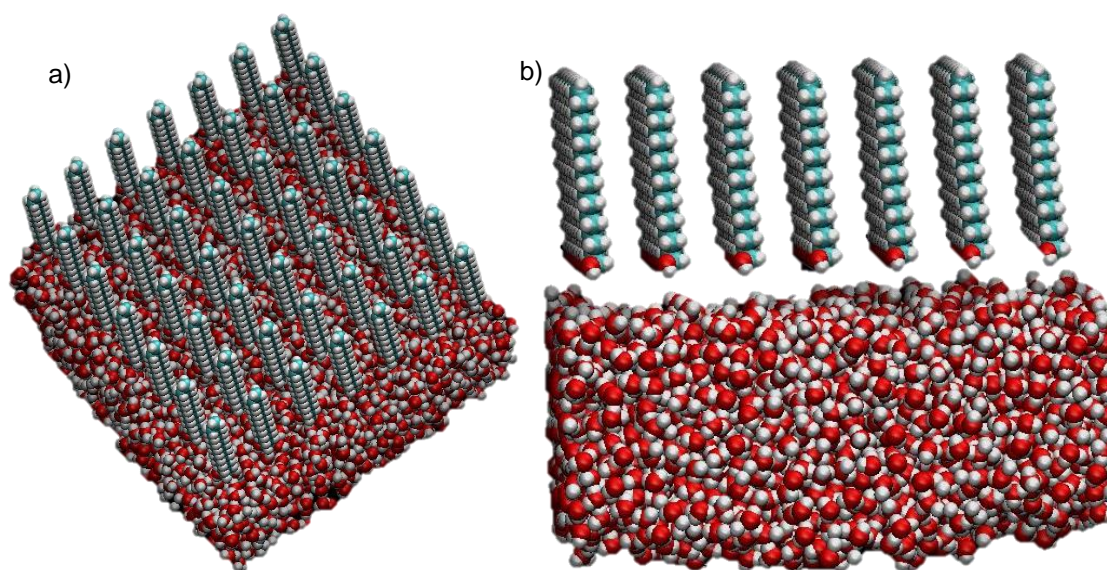


Figure 9 – Initial configuration of 18H above water, $93\text{\AA}^2/\text{molecule}$.

Trajectories were visualised using the VMD software, developed by Humphrey *et al.*^[36].

To quantitatively analyse the organization of the monolayer at the surface of water an order parameter was calculated, defined as follows. The orientation of each alcohol molecule was defined by calculating a normalized vector with origin at the oxygen atom and ending at the carbon atom of the terminal group. The order parameter, calculated for each time step, is defined as the average of the scalar product of the orientation vectors for each molecule pair,

$$O_u = \langle \vec{u}_i \cdot \vec{u}_j \rangle_{i \neq j}, \quad (6)$$

The order parameter can display values between -1 to 1. 1 indicates that all molecules are parallel to each other in the same direction. 0 represents a disordered monolayer.

3. Results and Discussion

3.1. Short chain Alcohols

3.1.1. Surface Tension of TFE as a function of Temperature

The surface tension of pure TFE was studied in a temperature range of 266.15K to 308.15K. The results are reported in Table 2 and plotted in Figure 10.

Table 2 - Surface Tension of TFE as a function of temperature.

EtOH	
T / K	γ / mN.m ⁻¹
266.15	22.33 ± 0.04
273.15	21.62 ± 0.06
278.15	21.25 ± 0.05
283.15	20.93 ± 0.09
288.15	20.50 ± 0.08
293.15	20.11 ± 0.09
298.15	19.63 ± 0.07
303.15	19.27 ± 0.09
308.15	18.83 ± 0.10

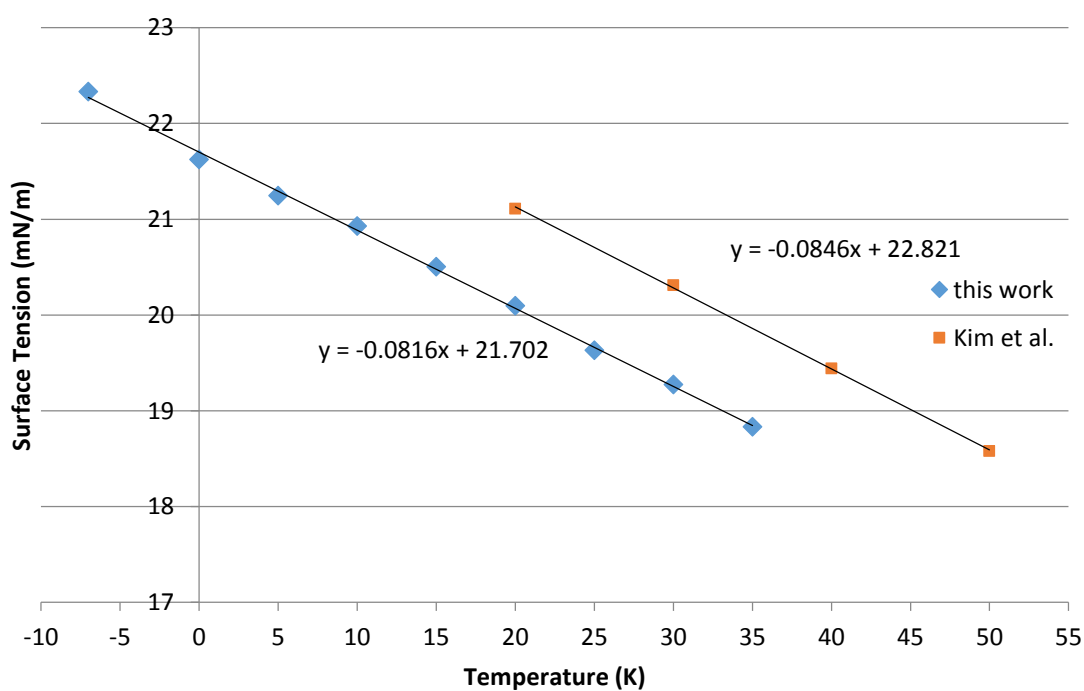


Figure 10 - Surface Tension of TFE as a function of temperature.

In Figure 10, our measurements are also compared with those of Kim *et al.* [37]. As can be seen, although the temperature dependence is very similar for both sets of results, our data are systematically lower (~5%). It should be mentioned that the results of Kim *et al.* were obtained using a different experimental method (Wilhelmy plate) and that their TFE was used as received, without further purification. Since TFE is highly hygroscopic, a small amount of absorbed water can easily explain the difference in surface tension.

3.1.2. Surface Tension of mixtures of Hydrogenated and fluorinated alcohols

Mixtures of TFE with ethanol, propanol, 1-butanol and tert-butanol were studied as a function of composition at 293.15K. The results are reported in Table 3 and plotted Figure 11.

Table 3 - Surface Tension of mixtures of ethanol, butanol, propanol and tert-butanol with 2,2,2-Trifluoroethanol, at 293.15K.

EtOH + TFE		PropOH + TFE		ButOH + TFE	
x TFE	$\gamma / \text{mN.m}^{-1}$	x TFE	$\gamma / \text{mN.m}^{-1}$	x TFE	$\gamma / \text{mN.m}^{-1}$
0	22.11 ± 0.09	0	23.68 ± 0.08	0	24.56 ± 0.10
0.101	21.20 ± 0.10	0.102	22.53 ± 0.08	0.100	23.44 ± 0.07
0.200	20.64 ± 0.10	0.199	21.67 ± 0.10	0.199	22.60 ± 0.09
0.301	20.06 ± 0.06	0.304	21.14 ± 0.06	0.304	21.85 ± 0.08
0.398	19.85 ± 0.08	0.399	20.72 ± 0.09	0.400	21.40 ± 0.09
0.493	19.78 ± 0.07	0.500	20.34 ± 0.05	0.494	20.95 ± 0.10
0.605	19.63 ± 0.06	0.601	20.00 ± 0.05	0.601	20.50 ± 0.07
0.699	19.68 ± 0.07	0.698	19.77 ± 0.06	0.699	20.16 ± 0.10
0.800	19.72 ± 0.10	0.800	19.80 ± 0.09	0.800	20.05 ± 0.09
0.900	19.88 ± 0.09	0.901	19.81 ± 0.06	0.871	19.91 ± 0.06
1	20.02 ± 0.05	1	20.02 ± 0.05	0.900	19.84 ± 0.05
				0.950	19.98 ± 0.06
				1	20.02 ± 0.05

Tert-ButOH + TFE	
x TFE	$\gamma / \text{mN.m}^{-1}$
0	20.57 ± 0.05
0.200	19.71 ± 0.07
0.401	19.27 ± 0.06
0.599	18.96 ± 0.05
0.799	19.09 ± 0.08
1	20.02 ± 0.05

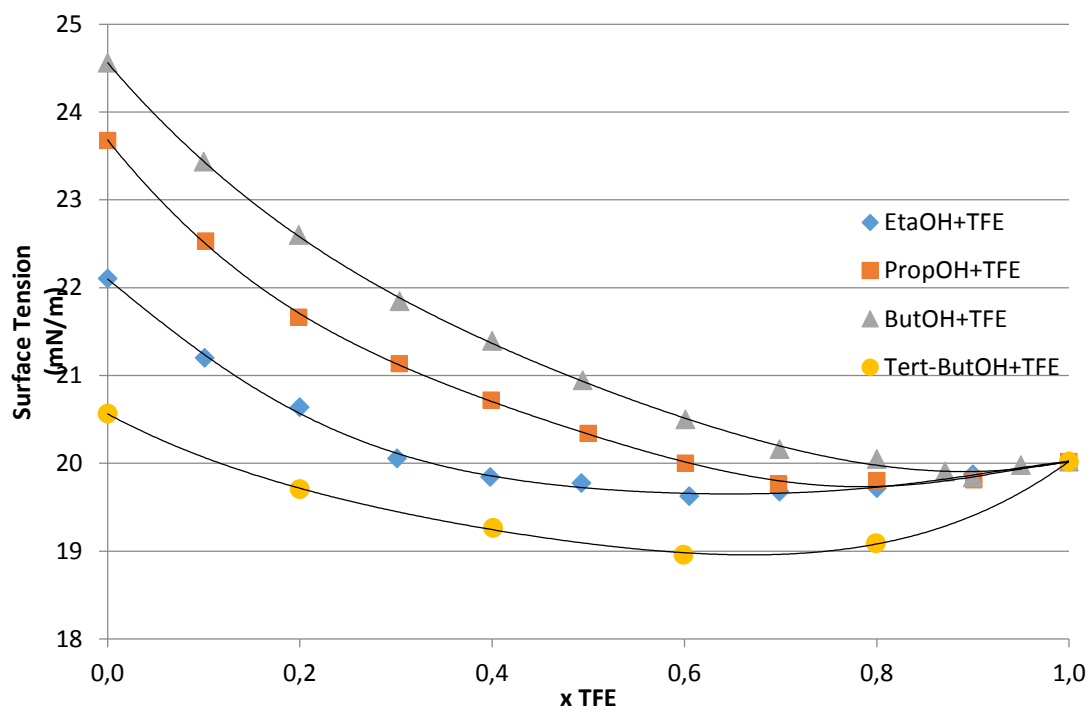


Figure 11 - Surface Tension of mixtures of hydrocarbon and fluorinated alcohols as a function of composition at 293.15K.

As expected the surface tension of hydrogenated alcohols increases with chain length. The measured values are in agreement with those reported in the literature [38-39]. Tert-Butanol is the only hydrogenated alcohol that does not follow this tendency.

All systems display minima in surface tension, more pronounced as the difference of surface tension between pure compounds decreases.

Mixtures richer in hydrogenated alcohols display a typical adsorption behaviour. The component with the lower surface tension (TFE) migrates to the surface in order to minimize the surface tension of the mixture.

Mixtures richer in TFE behave in a different way from what could be expected. Since TFE has the lowest surface tension it could be expected that these molecules would have the tendency to completely cover the surface, driving those of the hydrogenated alcohol to migrate from the surface to the bulk (due to its higher surface tension), remaining the surface tension of the mixture nearly constant. The experimental results show, however, that the presence of hydrogenated alcohol decreases the surface tension of the mixtures to values lower than either pure compound.

3.1.3. Excess molar volumes

The liquid densities of the mixtures of fluorinated and hydrogenated alcohols were also measured at 293.15K and atmospheric pressure. The corresponding excess molar volumes of the mixtures were calculated. The results are reported in Table 4 and plotted in Figure 13.

Table 4 - Densities and excess molar volumes of mixtures of ethanol, butanol, propanol and tert-butanol with 2,2,2- Trifluoroethanol, at 293.15K and atmospheric pressure.

EtOH + TFE			PropOH + TFE		
x TFE	$\rho / \text{g.cm}^{-3}$	$V_m^E / \text{cm}^3.\text{mol}^{-1}$	x TFE	$\rho / \text{g.cm}^{-3}$	$V_m^E / \text{cm}^3.\text{mol}^{-1}$
0	0.789307	0	0	0.803544	0
0.101	0.858907	0.249598	0.102	0.857607	0.324038
0.200	0.924094	0.504644	0.199	0.910191	0.543343
0.398	1.048504	0.668728	0.304	0.966505	0.800434
0.493	1.108507	0.730782	0.399	1.019619	0.930701
0.699	1.223735	0.640983	0.500	1.076537	1.076537
0.800	1.279807	0.503134	0.601	1.134665	1.061907
0.900	1.335541	0.307831	0.698	1.194491	0.872170
1	1.391144	0	0.800	1.256794	0.756041
			0.901	1.322145	0.477452
			1	1.391144	0

ButOH + TFE			Tert-ButOH + TFE		
x TFE	$\rho / \text{g.cm}^{-3}$	$V_m^E / \text{cm}^3.\text{mol}^{-1}$	x TFE	$\rho / \text{g.cm}^{-3}$	$V_m^E / \text{cm}^3.\text{mol}^{-1}$
0	0.809867	0	0	0.785879	0
0.100	0.852981	0.382623	0.200	0.876281	0.666249
0.199	0.898238	0.640571	0.401	0.977554	1.123200
0.400	0.99641	1.114869	0.599	1.092344	1.172092
0.494	1.047024	1.195166	0.799	1.227155	0.861379
0.601	1.10675	1.267111	1	1.391144	0
0.699	1.169234	1.073217			
0.800	1.235892	0.917172			
0.900	1.391144	0.548406			
1	0.852981	0			

The Redlich-Kister equation was fitted to the experimental results of the excess molar volumes.

$$V_m^E = x_1 x_2 \sum_k A_k (x_1 - x_2)^k \quad (7)$$

where V_m^E is the excess molar volume, x_i is the composition of specie I and A_k are adjustable coefficients. The adjustable coefficients of the Redlich-Kister equation are compiled in Table 5.

Table 5 - Redlich-Kister adjustable coefficients for mixtures at 293.15K and atmospheric pressure.

Mixture	EtOH+TFE	PropOH+TFE	ButOH+TFE	Tert-ButOH+TFE
A ₀	3.0219	4.1736	4.9289	4.7713
A ₁	-0.2683	-1.04	-1.2077	-0.9532

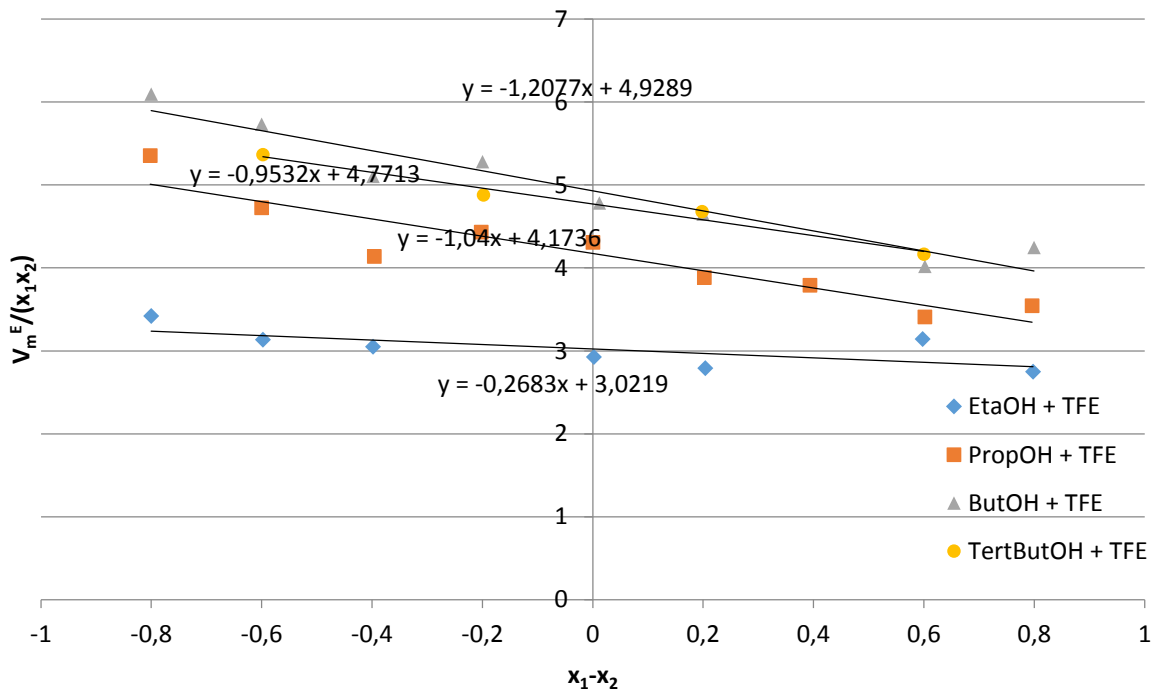


Figure 12 - Redlich-Kister Regressions.

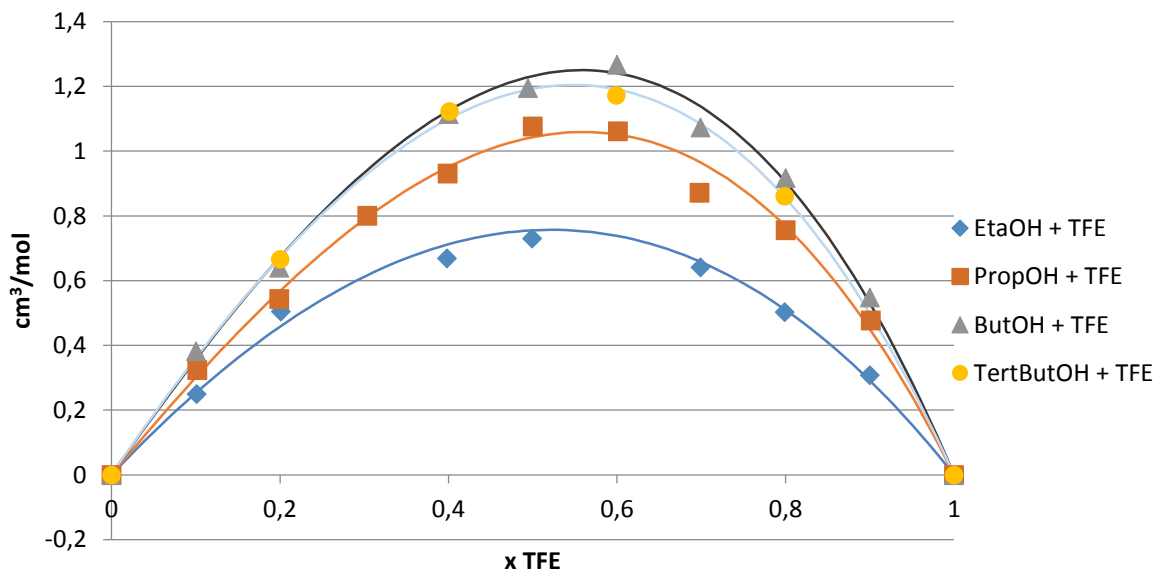


Figure 13 – Excess molar volume of hydrogenated alcohols and TFE mixtures. Points represent experimental results and the solid lines the Redlich-Kister equation.

As can be seen in Figure 13, the excess molar volumes of all mixtures are positive and increase as the chain length of the hydrogenated alcohol increases.

Mixtures of TFE with Ethanol, 1-Propanol and 1-Butanol have been studied by Atik *et al.*^[40,41]. Their results although obtained at a different temperature, 298.15K, (V_m^E $\frac{1}{2}$ ethanol = 0.8172 cm³ mol⁻¹, V_m^E $\frac{1}{2}$ 1-Propanol = 1.0192 cm³ mol⁻¹ and V_m^E $\frac{1}{2}$ 1-butanol = 1.0421 cm³ mol⁻¹) seem to agree with those obtained in this work.

3.1.4. Discussion

As previously explained, one of the objectives of this thesis is to understand the effect of mixing fluorinated and hydrogenated molecules that simultaneously associate through hydrogen bonding.

Due to its fundamental and technologic importance, mixtures of ethanol and TFE have been studied by a number of authors. Minamihonoki *et al.*^[42] measured the excess molar volumes and excess molar enthalpies. The former were found to be positive ($V_m^E_{1/2} = 0.8 \text{ cm}^3 \text{ mol}^{-1}$) and the later negative ($H_m^E_{1/2} = -700 \text{ J mol}^{-1}$). Smith *et al.*^[43] studied the vapour-liquid equilibrium of this system at 298.15K and found negative deviations to Raoult's law and a negative azeotrope at $x_{(\text{TFE})} = 0.4$. The simultaneous existence of a large positive excess molar volume and a large negative excess molar enthalpy (negative deviations to Raoult's law and a negative azeotrope) of mixing is a clear indication of the complexity of this binary mixture.

For comparison, it should be mentioned that mixtures of primary alcohols display positive excess molar volumes and enthalpies, which are very small when the alcohols have similar chain length and increase with the difference in chain length. Thus, the mixture of ethanol and TFE displays an opposite behaviour relatively to mixtures of hydrogenated alcohols. On the other hand, mixtures of alkanes and perfluoroalkanes exhibit large positive excess molar volumes and enthalpies^[16]. The negative excess enthalpy of the ethanol + TFE mixture is an indication of stronger cross interaction between the hydrogenated and fluorinated alcohols. The positive excess molar volume can be either a sign of less efficient packing or weaker interaction between the hydrogenated and fluorinated segments, as found for mixtures of alkanes and perfluoroalkanes.

As was seen in chapter 3.1.1 the surface tension as a function of composition of all studied mixtures displays a minimum. Minima in surface tension or aneutropes, denote a complex behaviour in the mixture, are relatively unusual and can be interpreted as an indication of low cohesion in the liquid-vapour interface. Nevertheless, aneutropes have been reported in the literature. Mclure *et al.*^[18] and Handa *et al.*^[18] reported aneutropes for mixtures of alkanes and perfluoroalkanes and Mejia *et al.*^[44] reported aneutropes for binary mixtures of ethanol with alkanes.

Aneotropes cannot be explained by the Gibbs adsorption equation (4). At the aneutrope, the concentration of both the bulk and surface, must be equal^[44]. Aneotropes are also frequently related with the proximity of an upper critical solution temperature (UCST)^[18,45]. Furthermore, in all systems reported in the literature displaying aneutropes, these can be interpreted as resulting from weak interactions between the two types of molecules in the bulk.

In the case of mixtures of hydrogenated and fluorinated alcohols, however, the interactions between the two components are rather strong as shown by their negative excess enthalpies. Moreover, all mixtures studied in this work demonstrated no sign of phase separation when cooled up to 193.15K or upon heating to 373.15K. In the bulk, hydrogen bonding dominates over the weak dispersion forces between hydrogenated and fluorinated chains^[17]. The existence of minima in the surface tension curves must be then related to weak surface cohesion. This suggests that the unfavourable coexistence of alkyl

and perfluoroalkyl segments, conditioned by the geometry of the interface, is not compensated by hydrogen bonding.

3.2. Long chain Alcohols

The behaviour of Langmuir films at the air-water interface of 18H, 18F, 14F and their mixtures was studied. The films were transferred to the surface of silicon wafers using the Langmuir-Blodgett technique and analysed by Atomic Force Microscopy (AFM). MD simulations were performed to obtain molecular level insight of the behaviour of the films of both pure species and mixtures.

3.2.1. Langmuir and Langmuir-Blodgett films

18F, 18H and (18F + 18H)

Langmuir isotherms of 18H, 18F and their mixtures were obtained at 293.15K and are shown in Figure 14.

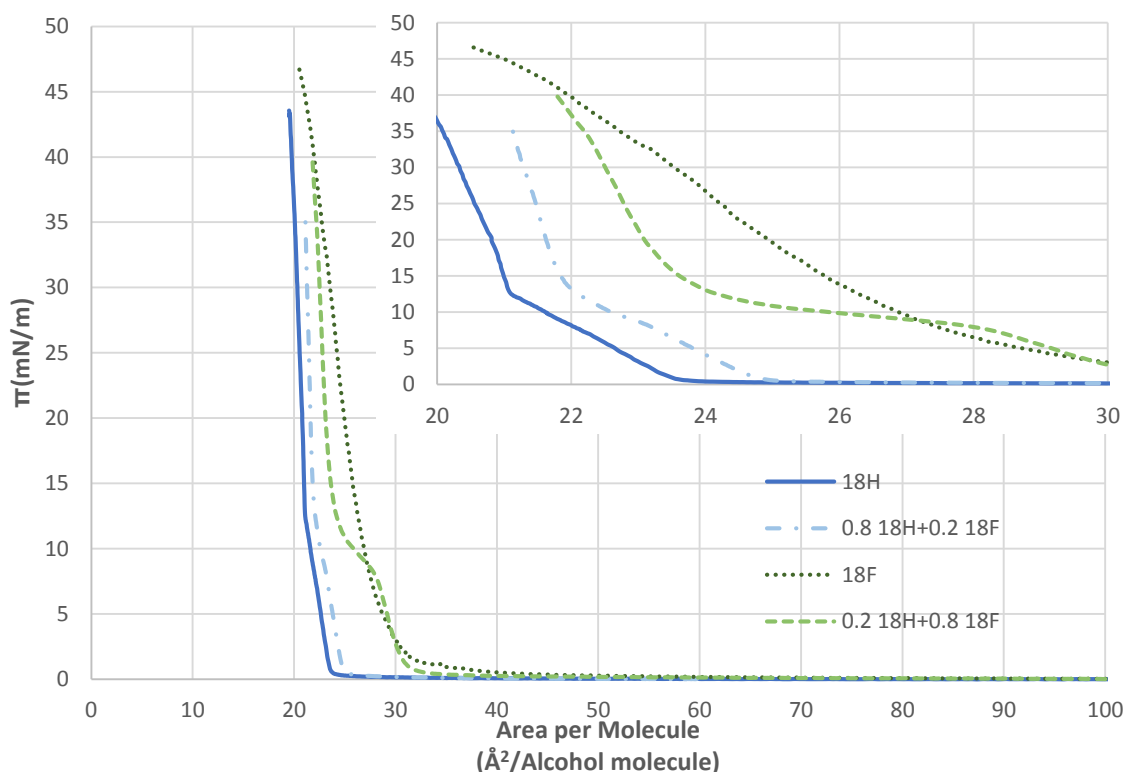


Figure 14 - Langmuir Isotherms of 18F and 18H, pure and mixtures, at 293.15K.

The results obtained for 18H has consistent with those from the literature [46]. There are three regions characterizing the 18H isotherm. A vapour-liquid expanded equilibrium plateau where π remains practically zero. A condensed tilted phase where the surface pressure starts to increase and the solid untilted phase after the inflection at 12mN/m.

18F displays a different behaviour in which only two regions are observed: a) a plateau at low π generally interpreted as a region of liquid-vapour equilibrium; b) a region of high surface density corresponding to a condensed monolayer, generally described as a hexatic phase.

The major difference, between 18H and 18F is the presence of a clear kink in the former, distinguishing the transition from a tilted to an untilted monolayer. Another important difference is the difference in the extrapolated areas to $\pi=0$ mN/m. While 18H has an area of $21.5 \text{ \AA}^2/\text{molecule}$, 18F has an area of $28.5 \text{ \AA}^2/\text{molecule}$. These results are coincident with the literature and with the cross section of hydrogenated and fluorinated chains.

As could be expected, the Langmuir isotherms of the mixtures are located between those of the pure alcohols. It should be noted that isotherms corresponding to an ideal 2D mixture and to a mixture that separates in two completely immiscibility phases will display exactly the same areas per molecule.

In order to obtain a deeper understanding of the structure of the Langmuir films, these were transferred to the surface of silicon wafers and analysed using Atomic Force Microscopy (AFM).

18F (0.8) + 18H

Figure 15 shows images from several AFM scans of a mixture richer in 18F (80%mol). It shows several hexagonal domains, the largest having between $2\mu\text{m}$ and $5\mu\text{m}$ width. Height profiles indicate that the average thickness of the film ranges between 1.7nm and 2.2nm , which is compatible with a monolayer. Small clusters with heights comparable with those of the hexagonal domains are also seen.

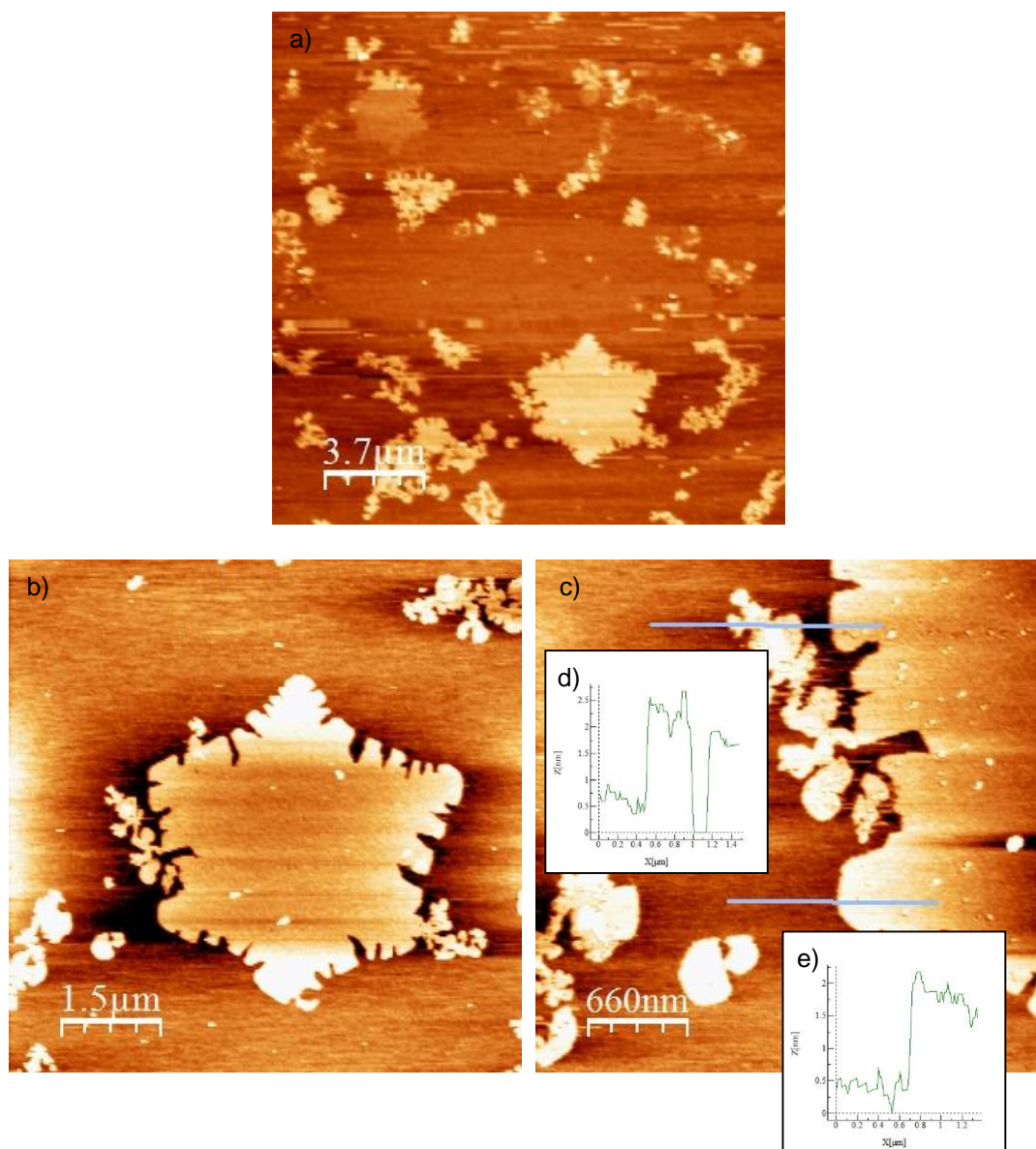


Figure 15– AFM scan of mixture between 18F and 18H (0.8-0.2) at $70\text{\AA}^2/\text{molecule}$ - topography contrast a), b) and c). d) and e) are height profiles.

18F + 18H (0.8)

Figure 16 shows the AFM image of a mixture richer in 18H (80%mol). In addition to the hexagonal domains, it also displays several circular domains between them. Hexagonal domains now have from $1\mu\text{m}$ to $3.5\mu\text{m}$ width. The height of the hexagonal domains are similar to those found on the 18F richer mixture.

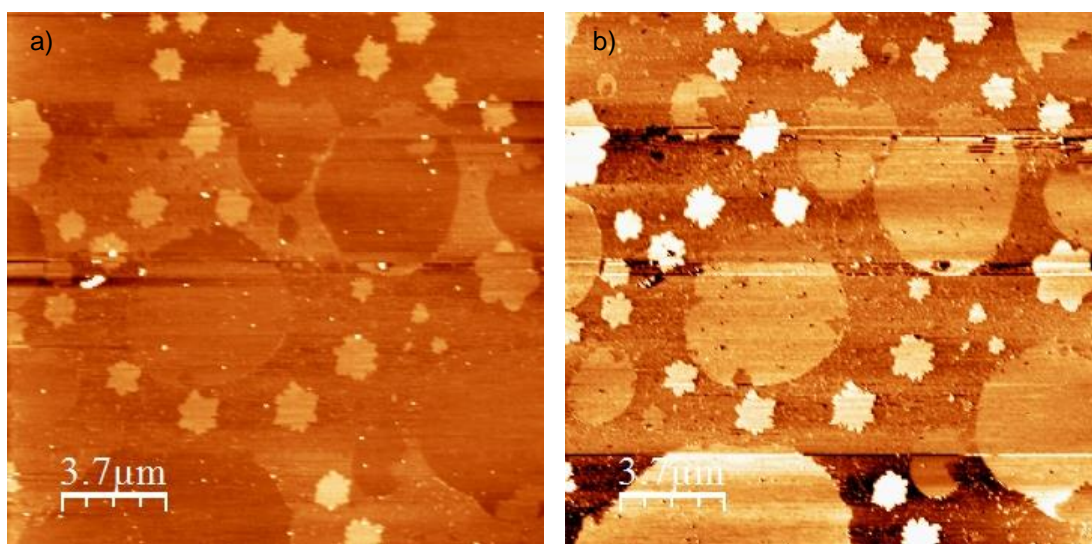


Figure 16– AFM scan of a mixture between 18F and 18H (0.2-0.8) at $70\text{\AA}^2/\text{molecule}$. a) topography and b) phase contrast.

Circular domains are commonly related to the presence of 2D liquids in Langmuir Films. Hydrogenated alcohols are known to form 2D liquids at room temperature [23]. The images show an additional interesting characteristic. The liquid circular domains seem to be surrounded by hexagonal domains, as if they were preventing them to coalesce.

The AFM scans clearly shows evidence of phase separation. Phase separation cannot be inferred by the Langmuir isotherms.

Pure 18H

Langmuir-Blodgett films of the pure alcohols were also produced and analysed by AFM. This was done to obtain a basis of comparison as no evidence of crystallization was expected in the pure films.

In Figure 17, the AFM scan of Langmuir-Blodgett film of pure 18H, shows a flat surface, suggesting that the coalescence of 18H 2D liquid domains produces a homogeneous surface. Several unsuccessful attempts were made in order to demonstrate the presence of circular domains at low pressure, at the vapour-liquid equilibrium region.

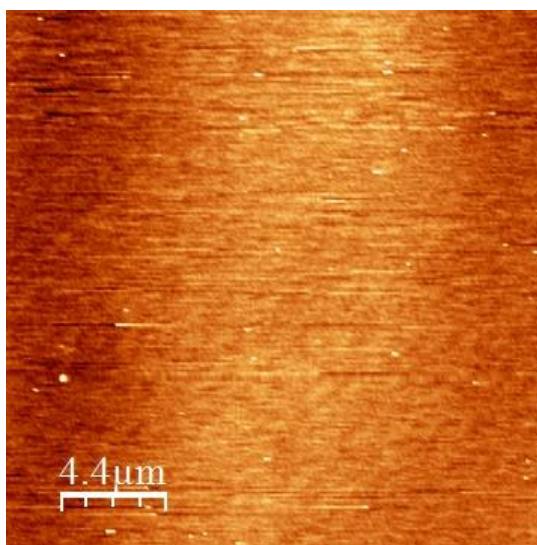


Figure 17 - AFM scan of pure 18H at $20.3\text{\AA}^2/\text{molecule}$ and 30mN/m - topography contrast.

Pure 18F

In Figure 18, the AFM scan of a Langmuir-Blodgett film of pure 18F deposited at $85\text{\AA}^2/\text{molecule}$ and $\pi=0\text{mN/m}$, is shown. The figure shows the existence of hexagonal / star shaped domains as well as smaller irregular shaped clusters, with height similar to those previously found. The largest hexagonal domain has $5.5\mu\text{m}$ width. This result clearly shows that the hexagonal domains form spontaneously in the film of pure fluorinated alcohol at $\pi=0\text{mN/m}$ and that the presence of the hydrogenated alcohols (18H) is not needed to induce the nucleation of hexagonal domains. It also suggest that the composition of the hexagonal domains observed in the mixtures should be predominantly composed by 18F.

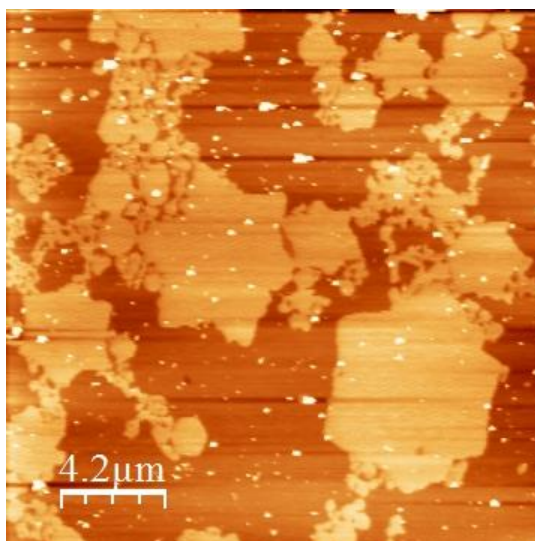


Figure 18 – AFM scan of pure 18F at $85\text{\AA}^2/\text{molecule}$ - topography contrast.

14F, 18F and 18F + 14F

In order to obtain a deeper understanding of the 2D crystallization of pure fluorinated alcohols, Langmuir films of a fluorinated alcohol with a shorter chain were studied. It is interesting to note that this is equivalent to increasing the reduced temperature.

The Langmuir isotherms of 14F, 18F and a $x(18F)=0.8$ mixture of the two alcohols, are shown in Figure 19. The isotherm of pure 14F is more expanded than that of 18F, which is consistent with literature results [46]. The isotherm of the mixture is very close to that of pure 18F.

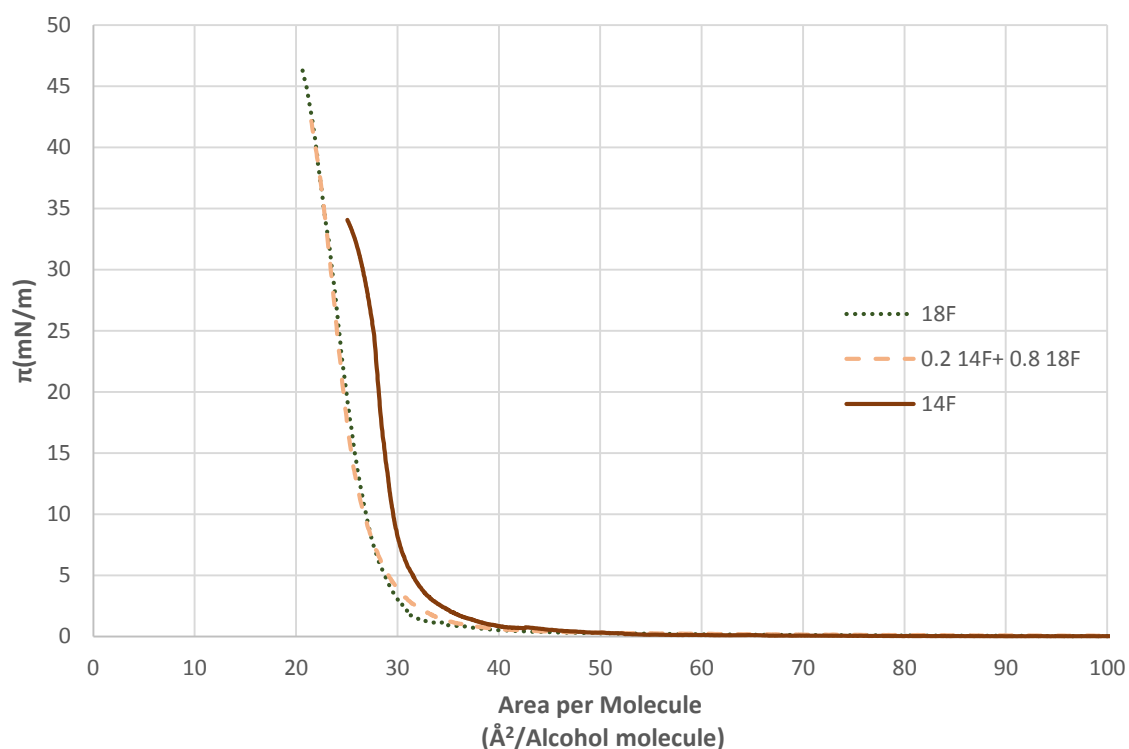


Figure 19 - Langmuir balance Isotherm of 18F and 14F, pure and mixtures, at 293.15K.

Pure 14F

In Figure 20 the AFM scan of Langmuir-Blodgett film of pure 14F is shown. As can be seen, it displays a completely different type of pattern from what has been observed until now. These “lacy” type structures are approximately 2nm high. The open structure of the domains and the absence of regular shapes suggests lower tendency to accrete or crystalize.

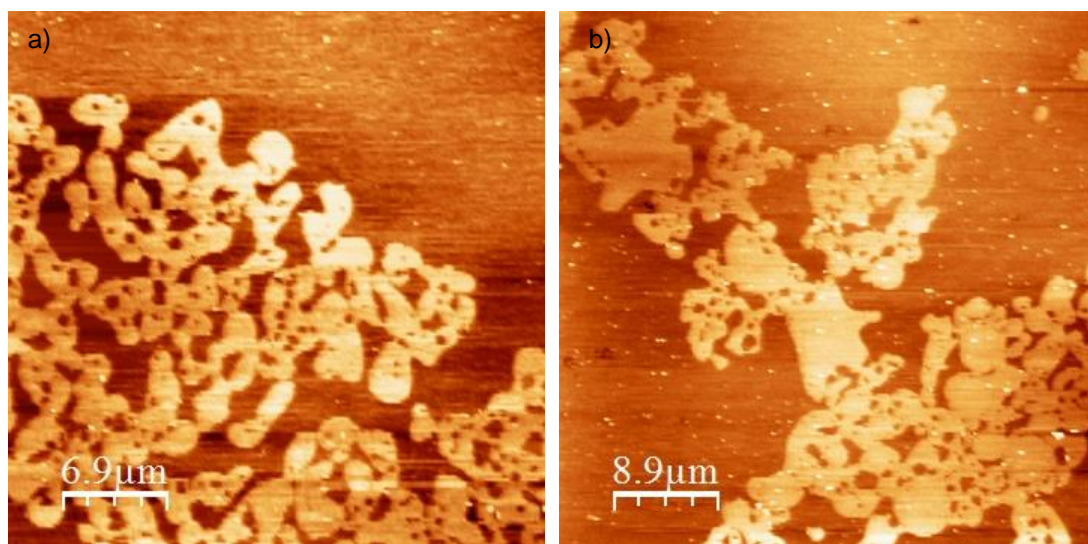


Figure 20 - AFM scan of pure 14F at $70\text{\AA}^2/\text{molecule}$ – topography contrast.

18F (0.8) + 14F

Figure 21 shows the AFM scan of a Langmuir-Blodgett film of a mixture of 18F and 14F alcohols.

As can be seen the image shows an intricate structure that seems to combine the domains observed in the films of pure 18F and 14F. Hexagonal domains are clearly seen, having attached strands that could be considered reminiscent of the “lacy” structures found in the films of pure 14F. The height of both types of structures is similar to those observed before (1.5-2.2nm).

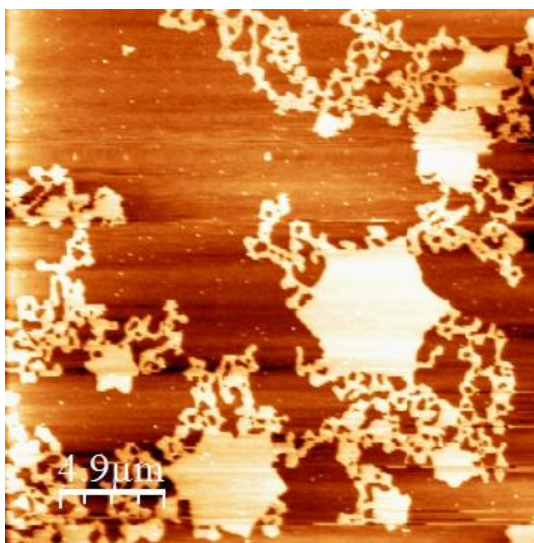


Figure 21 - AFM scan of mixture between 18F and 14F (0.8-0.2) at $80\text{\AA}^2/\text{molecule}$ – topography contrast.

Temperature Influence on 18F and 14F

Langmuir and Langmuir-Blodgett films of 14F and 18F were studied as a function of temperature (278.15K and 308.15K).

Performing experiments as a function of temperature in Langmuir film balances can be quite challenging. Given the geometry and the material from which Langmuir troughs are made, an accurate temperature control can be difficult. Langmuir troughs are usually made from Teflon, which has a low heat transfer coefficient, thus temperature stabilization becomes difficult to achieve. At low temperatures, around 278.15K, the temperature gradient inside the Langmuir balance, after several hours, was found to be at least of the order of 2K. Lower temperatures could not be achieved because water started to freeze. Temperatures higher than 308.15K are difficult to use due to high evaporation of the subphase.

In Figure 22 the AFM image of a Langmuir-Blodgett film of pure 18F obtained at 308.15K is shown. The system displays predominantly circular domains, very polydisperse. The larger domains are 2.5 μm width and are still hexagonal although displaying much smoother edges than the hexagonal domains found at 293.15K. The height of the domains was found to be similar to those found at lower temperatures (1.5-2nm).

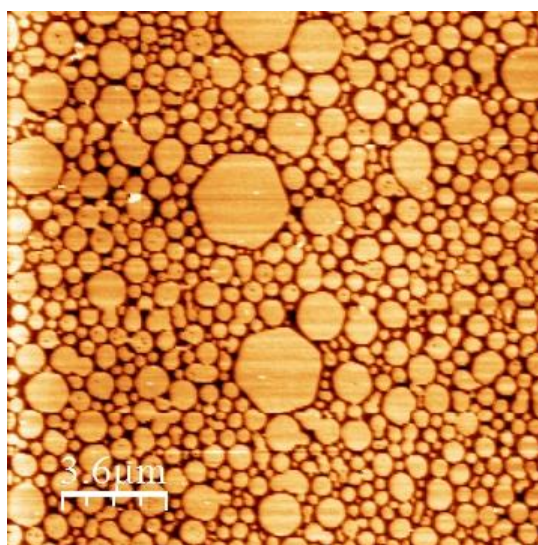


Figure 22 - AFM scan of pure 18F at $30\text{\AA}^2/\text{molecule}$ and 5mN/m and 308.15K – topography contrast.

The AFM image of a Langmuir-Blodgett film of pure 18F obtained at 278.15K is shown in Figure 23. As can be seen, at this temperature the domains are star-shaped, with sharp edges, with a maximum width of $1.5\mu\text{m}$.

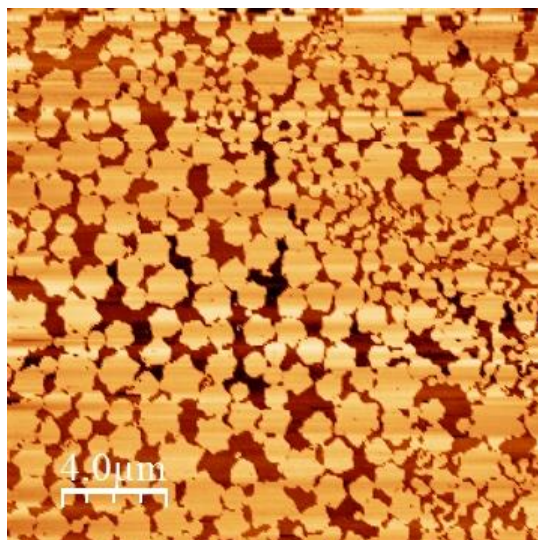


Figure 23 - AFM scan of pure 18F at $35\text{\AA}^2/\text{molecule}$ and 5mN/m and 278.15K – topography contrast.

It was noticed that the Langmuir isotherms are displaced to larger areas as the temperature decreases. This seems to be consistent with what is observed in Figure 22 and Figure 23: at the same surface pressure, the free area increases at lower temperatures. In fact, in Figure 22 the hexagonal domains are very close to each other, touching by edges, while in Figure 23 the hexagonal domains are well separated from each other, touching by the vertices. These findings deserve further confirmation.

Finally, in Figure 24 the AFM image of a Langmuir-Blodgett film of pure 14F obtained at 278.15K is shown. As can be seen, at this temperature the “lacy” structures observed at 293.15K (Figure 20) transformed into well individualized geometric domains, almost hexagonal.

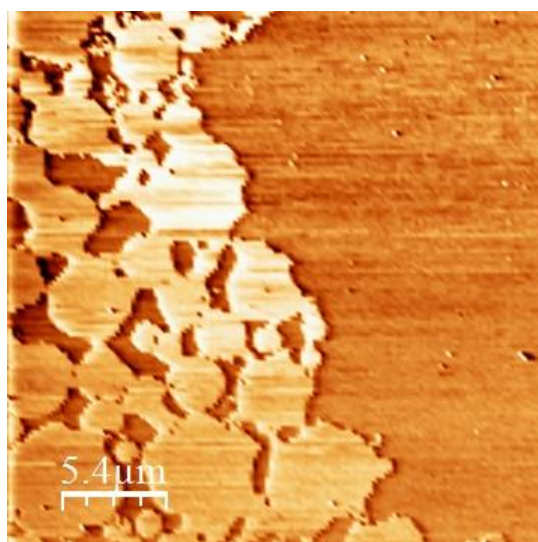


Figure 24 - AFM scan of pure 14F at $32\text{\AA}^2/\text{molecule}$ and 5mN/m 278.15K – phase contrast.

Evaporation Casting of pure 18F on silicon

Figure 25 shows the AFM image of a film of pure 18F produced with a different procedure. The film was obtained by spreading drops of the 18F solution directly on the surface of the dry hydrophilic silicon substrate. The amount of 18F deposited was consistent with the formation of a close-packed monolayer. The picture shows a highly dense pattern of hexagonal shapes with a regular size and distribution.

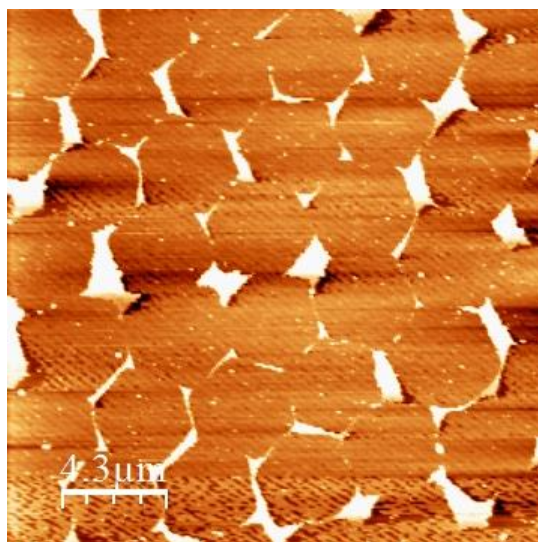


Figure 25 - AFM scan of pure 18F by evaporation casting – phase contrast.

3.2.2. Molecular Dynamics Simulations

MD simulations of Langmuir films of 18H, 18F and 14F and their mixtures were performed as a function of temperature (278.15K – 308.15K).

The purpose of performing these simulations was to obtain molecular level insight into the studied systems, in particular, to obtain arguments in favour of a particular type of organization at the surface of water. It is important to stress that the simulation results were not used to obtain quantitative estimations of the properties of the system, as much larger systems and simulation runs, would probably be required.

The simulations were conducted with the purpose of finding answers to three specific aspects experimentally found:

- 1- Do fluorinated alcohols have an enhanced tendency, as compared to their hydrogenated analogues, to spontaneously form highly organized aggregates (2D crystals) at the surface of water, even at very low surface coverage?
- 2- How does this tendency depends on chain length and temperature?
- 3- Do mixtures of fluorinated and hydrogenated alcohols tend to spontaneously phase separate at the surface of water?

To answer question 1, MD simulations of Langmuir films of 18F and 18H were performed. As explained in section 2.5, these simulations started with initial configurations formed by an array of regularly distributed parallel 18F and 18H molecules parallel to each other, placed over a 3.2nm layer of equilibrated water molecules (4000 molecules). The average density of alcohol molecules was quite low, approximately $93\text{\AA}^2/\text{molecule}$.

In Figure 26, a snapshot is shown of the simulation boxes of 18F and 18H at 25ps simulation time. As can be seen, both 18F and 18H molecules have clustered together and float at the surface with their OH groups in contact with water and the hydrophobic chains perpendicular to the surface. However, already at this short simulation time, the two systems display very different structures in terms of organization. 18F chains seem to be in a strait conformation, essentially parallel to each other, forming a highly organized structure. The hydrogenated chains of 18H on the contrary, seem to be much disorganized relatively to each other, many of them parallel to the surface and displaying numerous bend conformations. These findings agree with the known flexibility of hydrogenated chains as opposed to the rigidity of fluorinated chains.

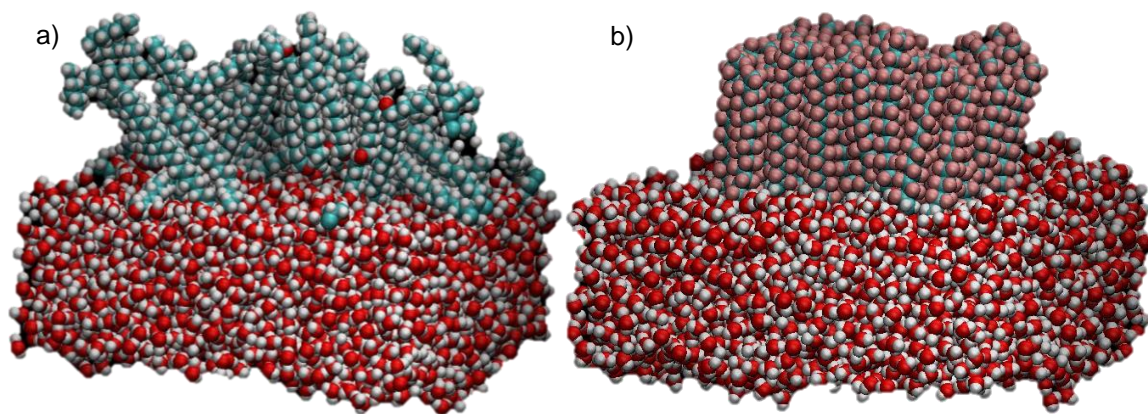


Figure 26 – a) 18H and b) 18F, above water after 25ps of simulation time.

In Figure 27 and Figure 28, sequences of snapshots at different simulation times, show the evolution of films of 18H and 18F, respectively. The total simulation time is 5ns, but the overall structure of the films seems not to change after 1-2ns.

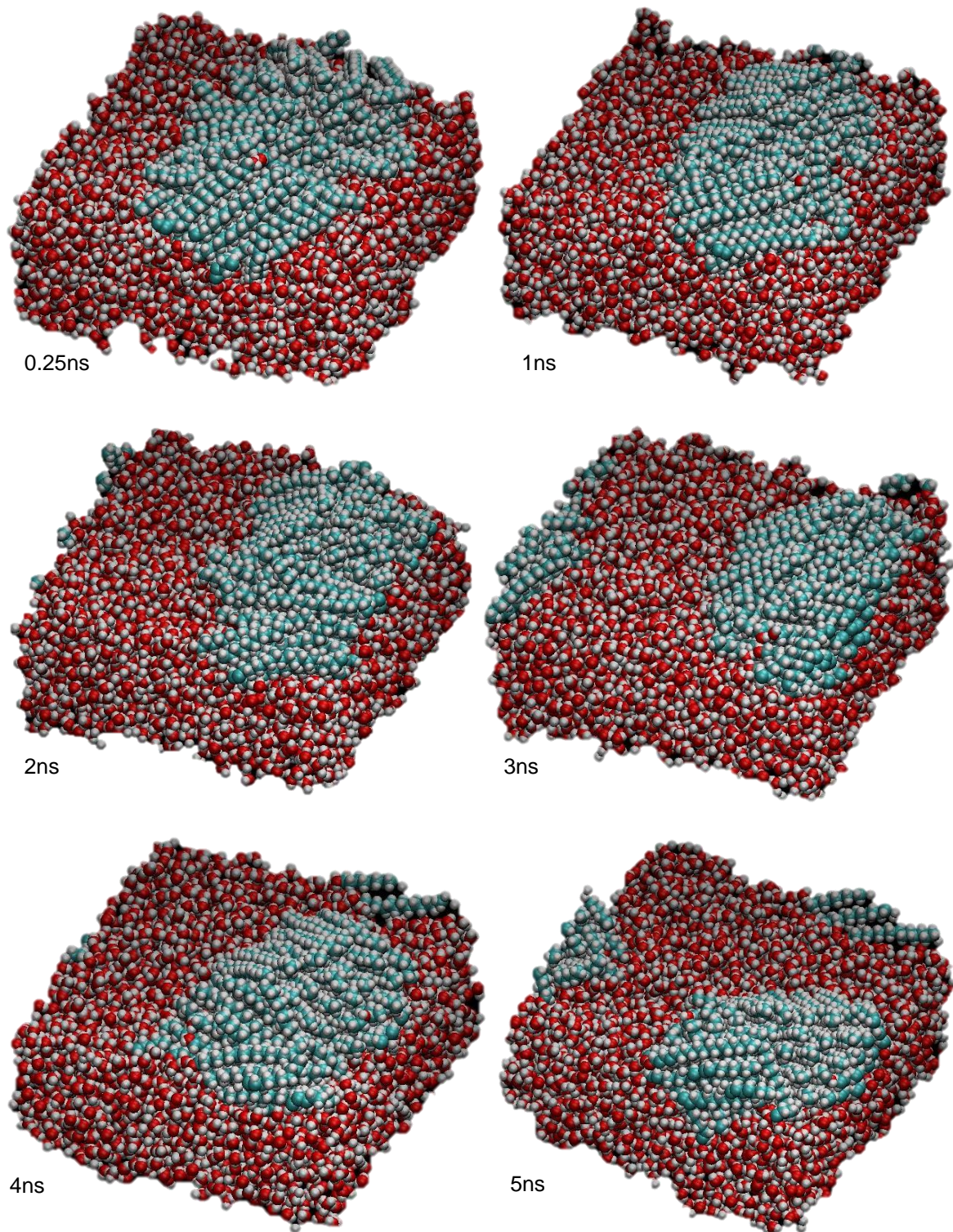


Figure 27 - Snapshots of 18H simulation during 5ns.

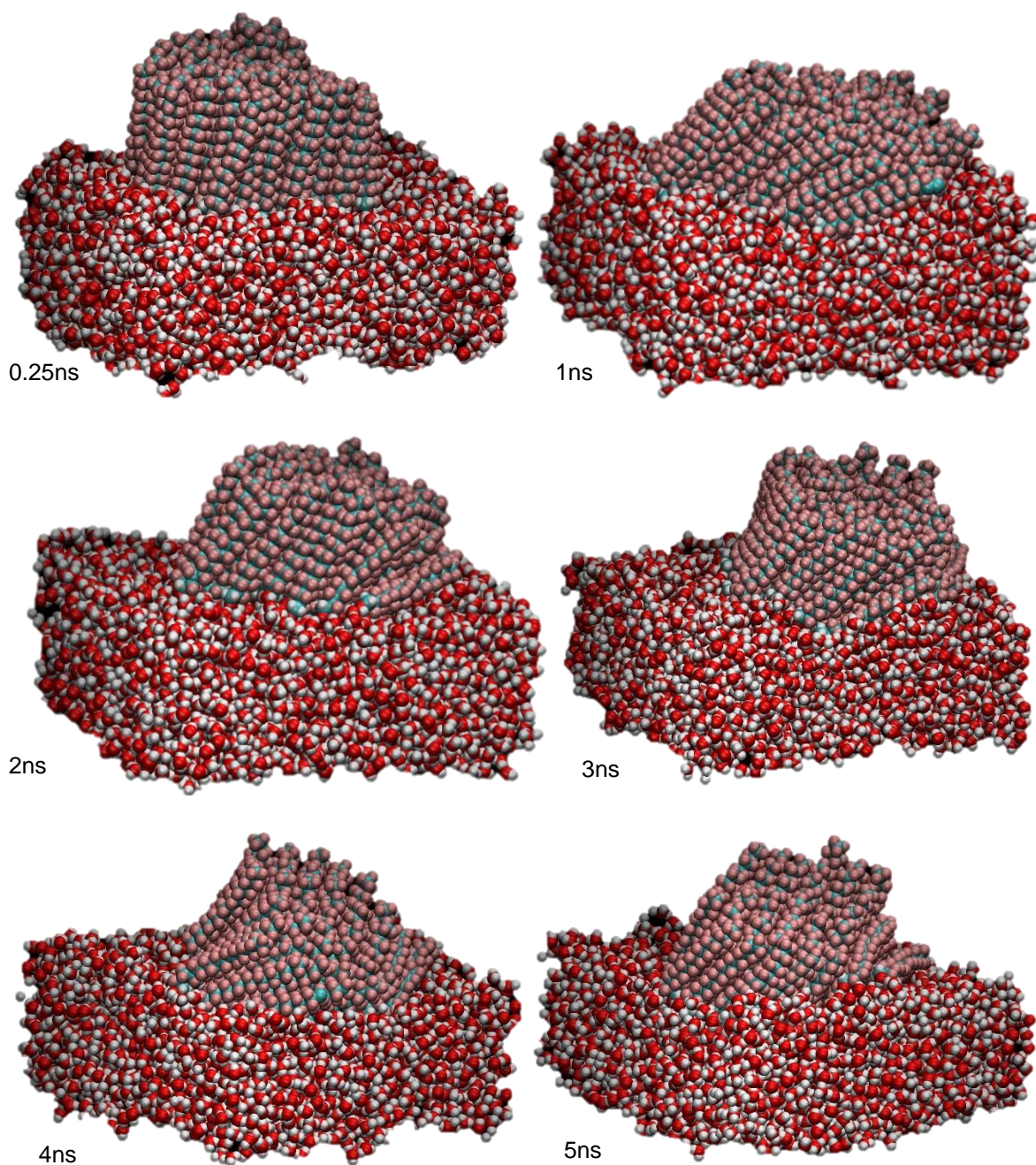


Figure 28 – Snapshots of 18F simulation during 5ns.

As can be seen, the hydrogenated chains of 18H form what seems to be a disorganized liquid like domain. Most chains lie parallel to the surface and display numerous bend conformations.

As previously described, 18F molecules immediately form a highly ordered structure, with almost all molecules parallel to each other and essentially perpendicular to the surface of water. After that, the film moves and tilts at the surface of water but the overall organization of the film seems to remain essentially intact throughout the simulation.

18F presents a hexatic molecular arrangement that can be examined in more detail in Figure 29. Two planes can be devised, one containing all OH groups and the other containing the carbon atoms of

terminal CH₃ groups (CT). Both planes are parallel and this alignment persists during the simulation. In the vertical projection the hexagonal structure of 18F film is clearly seen. Each molecule is surrounded by six molecules and this order extends throughout the structure. This structure is maintained during the simulation and can be related with the macroscopic hexagonal shapes of 18F, described in 3.2.1.

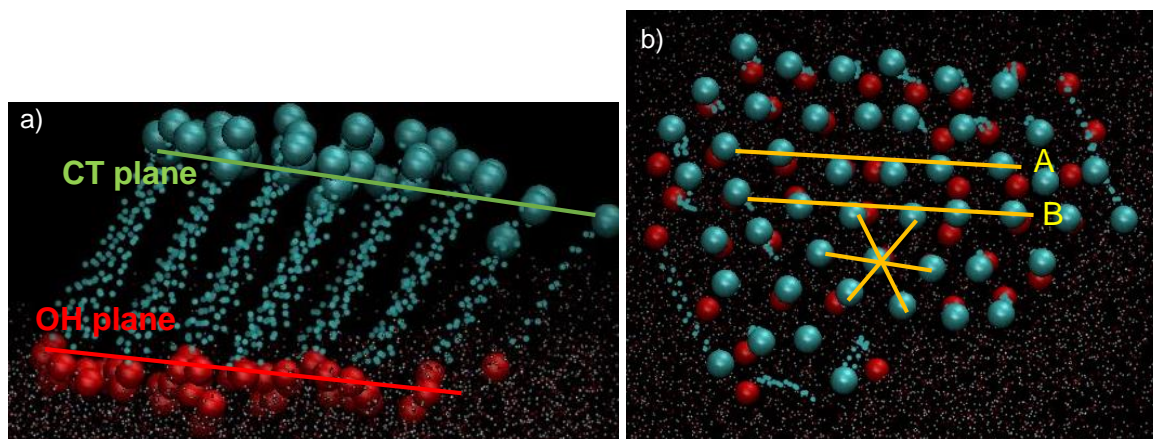


Figure 29 – a) Lateral and b) vertical projections of 18F. Red spheres represent oxygen atoms of OH groups. Blue spheres represent the carbon atoms terminal CH₃ groups.

In conclusion, the simulations seem to provide evidence of the tendency of long chain fluorinated alcohols to spontaneously form highly organized aggregates at the surface of water in agreement with the experimental observations. In order to evaluate the influence of chain length on the formation of these aggregates, equivalent MD simulations of 14F films were also performed. The results are shown in Figure 30.

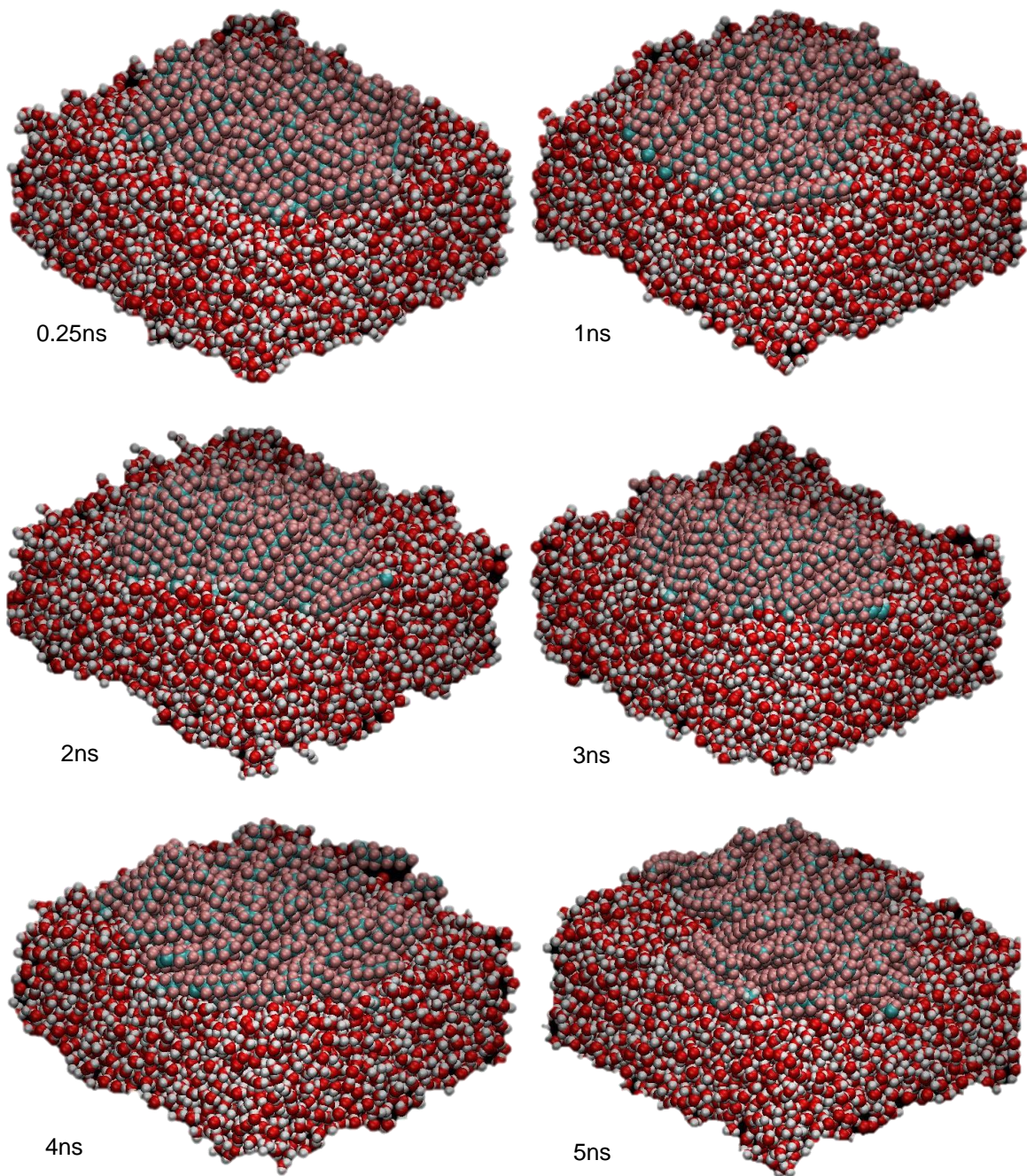


Figure 30 - Snapshots of 14F simulation during 5ns.

The overall behaviour of the 14F film can be considered very similar to that of 18F just described, but there are differences that are noteworthy. These are better appreciated in Figure 31 and Figure 32. As can be seen in the vertical projection of Figure 31, although each molecule is still locally surrounded by six other molecules, the longer range ordering is less apparent than in the case of 18F.

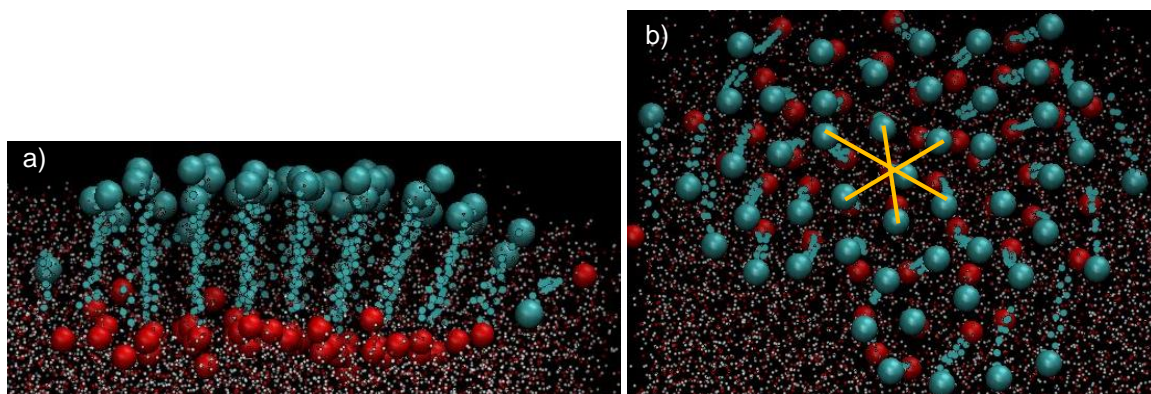


Figure 31 – a) Lateral and b) vertical projections of 14F. Red spheres represent oxygen atoms of OH groups. Blue spheres represent the carbon atoms terminal CH3 groups.

In Figure 32 the average order parameter of all studied films is shown as a function of simulation time. The order parameter is a measure of how parallel the molecules are to each other within the film and was calculated as explained in chapter 2.5.

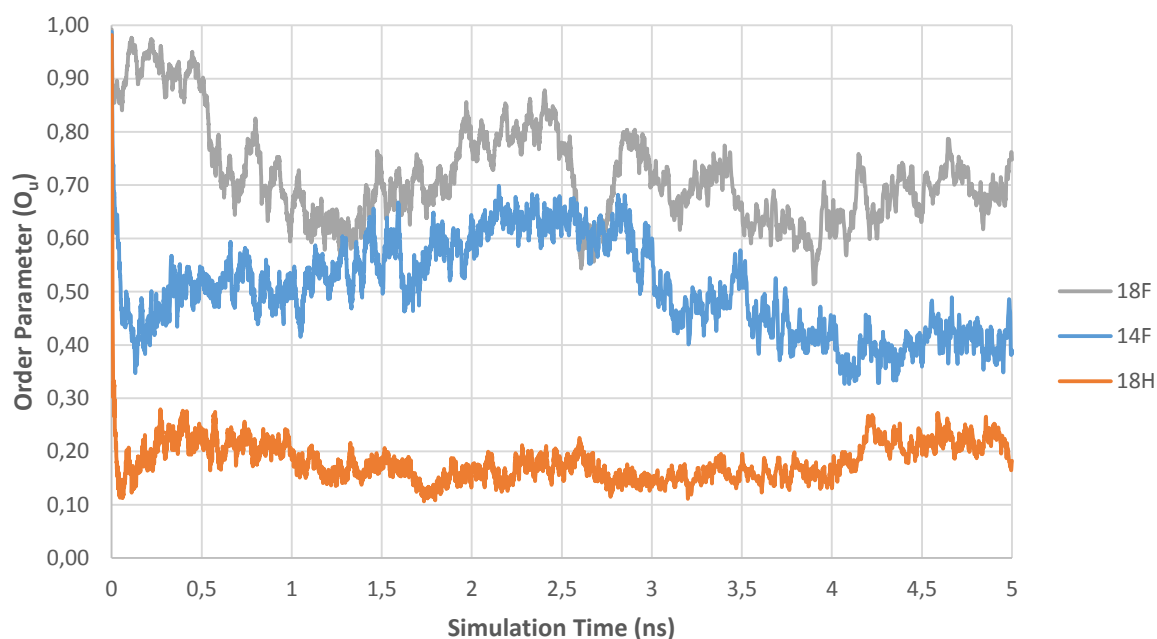


Figure 32 – Evolution of order parameter of Alcohols (18F, 14F, 18H) molecules in time.

The results shown in Figure 32 clearly show that the films formed by fluorinated chains are considerably more organized than that formed by hydrogenated chains. It is also seen that the longer the fluorinated chain the higher the order. These results are likely to be related to the tendency of 18F to form solid-like domains at the surface of water.

As evidenced in Figure 33, it was found that films of both 18F and 14F tend to be slightly tilted relative to the surface of water, i.e., partially submerged. It is important to note that this happens to the film as a whole and it's not likely to be related to potential dissolution of the film, as no sign of dissolution of individual molecules was found. The slight immersion of the film reduces the total area of the interface thus reducing the energy of the system and this is probably the origin of the effect. It is possible that in larger systems the relative contribution to the lowering of the free energy resulting from this decrease of the total surface is small. This could not be tested as, due to hardware limitations, the simulation boxes could not be enlarged. However, since all systems were simulated with boxes of the same size, the contribution of this effect should be similar in all cases.

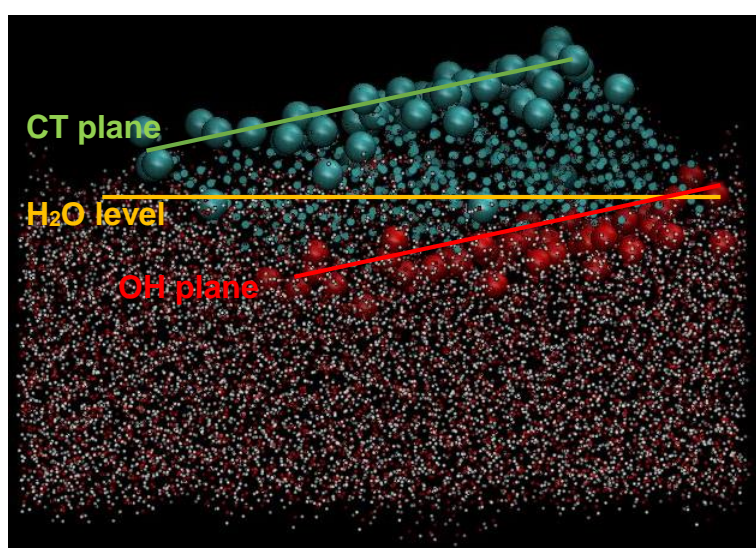


Figure 33 – 14F immersion on water.

An attempt was made to assess the influence of temperature on the organization of the films of pure fluorinated alcohols. Simulations, of 14F and 18F were performed at different temperatures (278.15K, 293.15K and 308.15K). The results are shown in Figure 34 and Figure 35, where the order parameter of the films at each temperature is plotted as function of simulation time. As can be seen, no significant differences were found, i.e., the order parameter doesn't change with temperature in the simulation conditions. Temperatures were not changed more significantly due to water evaporation and freezing.

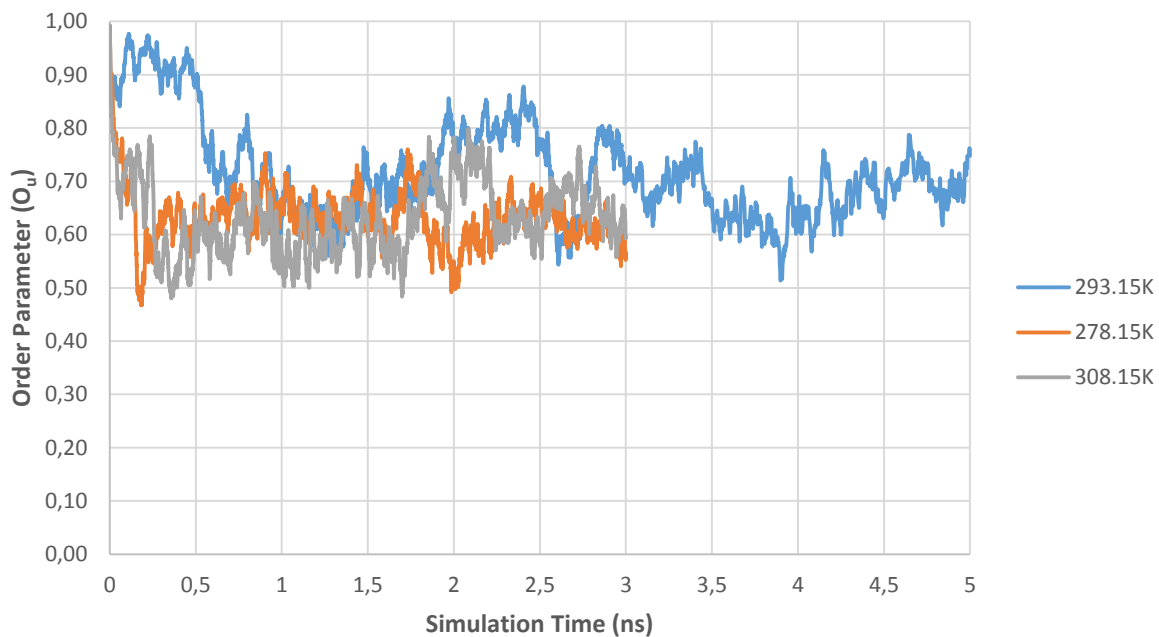


Figure 34 - Evolution of the order parameter of 18F at different temperatures in time, 278.15K, 293.15K, 308.15K.

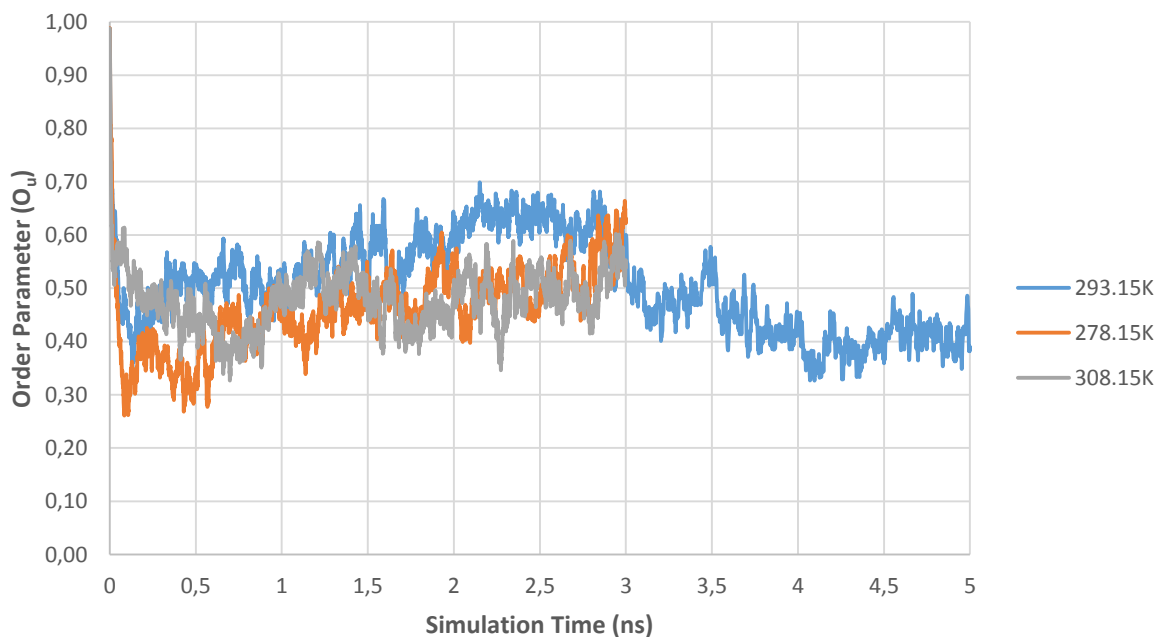


Figure 35 - Evolution of the order parameter of 14F at different temperatures in time, 278.15K, 293.15K, 308.15K.

18F + 14F and 18F + 18H

Finally, equimolar mixtures of fluorinated and hydrogenated alcohols were simulated in order to assess their tendency to spontaneously phase separate at the surface of water. Equimolar mixtures of the two fluorinated alcohols, 14F and 18F, were also simulated, as experimentally it is found that the two substances crystallize separately. Additionally, this could also provide insight about the mutual diffusion of the molecules within the film.

In the initial configuration of the mixture (Figure 36), molecules were positioned in a checkerboard pattern in order to make the mixture as homogenous as possible, although this may not be entropically the most favourable configuration.

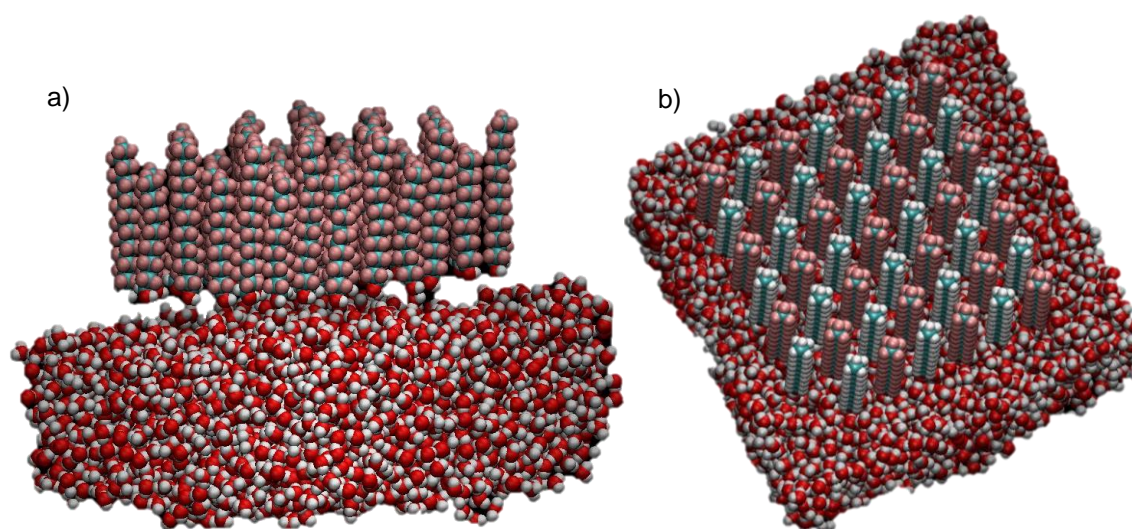


Figure 36 – a) Initial configuration of 18F + 14F mixture. b) Initial configuration of 18F + 18H mixture.

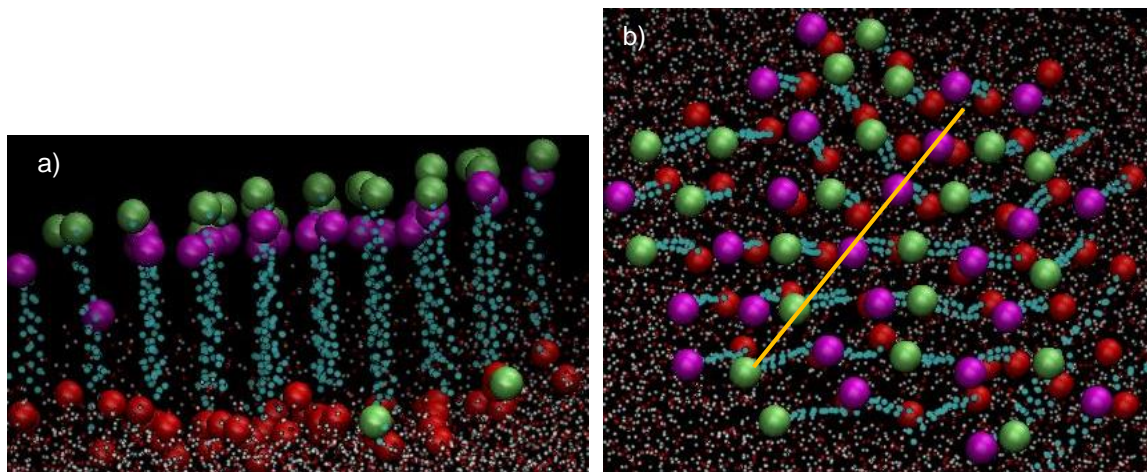


Figure 37 – a) Lateral and b) vertical projections of 18F-14F mixture, after 3ns. 18F are represented with terminal Carbon as Green and 14F with terminal Carbon as purple. The yellow line in Figure 37 b) represents the vertical plane observed in Figure 37b.

Figure 37 shows the vertical and lateral projections of the 14F+18F mixture. As can be seen in the vertical projection, the initial configuration (checkerboard) is only partially maintained. This seems to result from distortion of the planes of each alcohol, rather than from diffusion of the individual molecules. In Figure 39 the order parameter of this mixture is represented. As can be seen, it is practically identical to that of the pure 18F film. This is an indication that the network of 18F molecules is able to “absorb” a similar number of 14F molecules and maintain most of their characteristic order. The molecules remain parallel to each other, independently of the differences in chain length and in spite of the reduction in chain cohesion.

In the case of the mixture of 18F + 18H, the projection shown in Figure 38 indicates that the distortion of the initial configuration is much more pronounced. The initial planes of each type of alcohol are now difficult to identify. Nevertheless, the disordered liquid-like structure characteristic of the pure hydrogenated alcohol is completely absent as shown by the order parameter plotted in Figure 39. As can be seen, this very similar to that of pure 18F, suggesting that the fluorinated molecules are supporting the hydrogenated molecules. Within the simulation time, no evidence was found to the formation of segregated fluorinated and hydrogenated domains. It is likely that a much larger system would be necessary, as well as a quantitative criterion to identify the segregated domains.

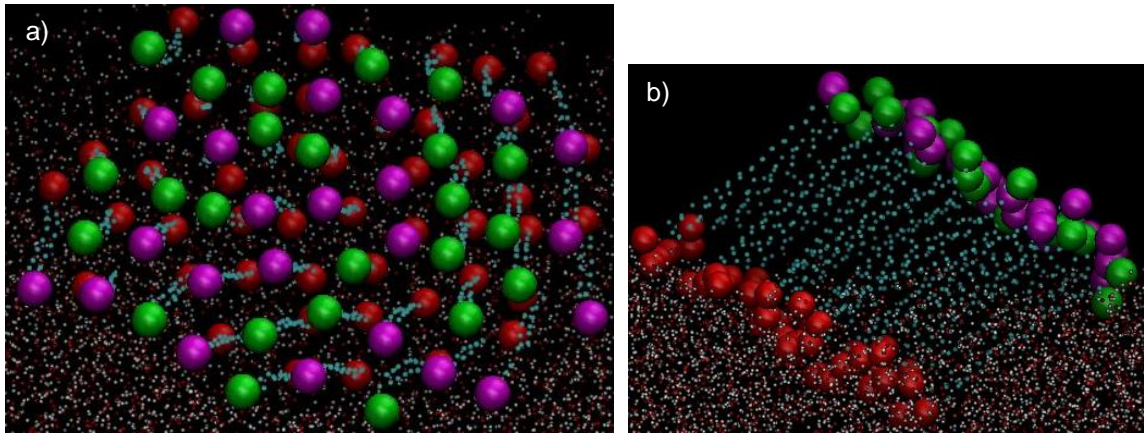


Figure 38 – a) Lateral and b) vertical projection of 18F-18H mixture, after 3ns. 18F are represented with terminal Carbon as Green and 18H with terminal Carbon as purple.

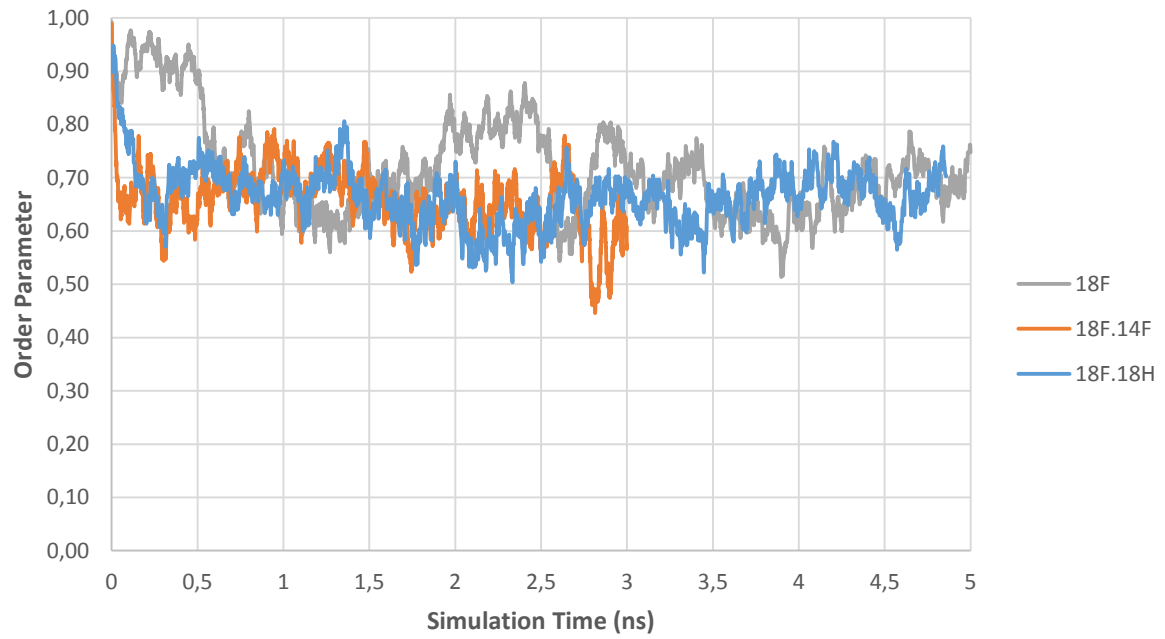


Figure 39 – Order Parameter as a function of time for both mixtures, 18F-14F and 18F-18H.

3.2.3. Additional remarks

One of the most important results of this work has been the observation of hexagonal domains in films of 18F at low surface density. Given their regular geometric shape, it is likely to assume that these domains are 2D crystals. The domains were observed at virtually zero surface pressure and very low surface density. It is thus reasonable to assume that, at this stage, the film is at a solid-vapour equilibrium region. These observations seem to indicate that long chain fluorinated alcohols tend to spontaneously crystalize at the surface of water.

Contrarily to what is observed in the isotherms of long chain hydrogenated alcohols (e.g. 18H), in which a sharp “kink” signals the transition from a condensed to a solid phase, in the isotherm of 18F there is a gradual increase of surface pressure that should correspond to the compression of solid domains against each other.

The influence of temperature on structure of the films corroborates what has been proposed. At a higher temperature, 18F films displays predominantly circular domains, very polydisperse, and the remaining hexagonal domains show much smoother edges than those found at 293.15K. The film is now at a liquid-vapour boundary. At lower temperature the domains are again predominantly star-shaped, as seen in Figure 23. The existence of a 2D triple point is inferred.

Studies involving a fluorinated alcohol with a smaller chain length (14F) attested and reinforced previous arguments. It is important to stress that smaller chains imply less cohesive energy within the film and thus higher reduced temperature.

At room temperature and low surface density, 14F films do not exhibit the geometric shaped domains that identify the solid-vapour equilibrium. Although the displayed “lacy” structure is difficult to ascertain to a liquid phase, at lower temperature it transforms into distinct solid like hexagonal domains. It is thus reasonable to conclude that at low temperature the 14F films is at a solid-vapour equilibrium region, while at higher temperature it is probably at or near to liquid-vapour boundary.

A closer analysis of the distribution of sizes and shapes of the observed domains can be useful to provide information about the possible mechanisms of domain growth.

It is known that crystalline structures grow more rapidly along the most compact directions. As shown in Figure 40, directions a_1 , a_2 and their family $-a_1$, $-a_2$, $-a_1+a_2$ and a_1-a_2 , are the most compact directions in a hexagonal lattice. This explains the existence of star shaped domains, as observed in the films of 18F. At low temperatures, as diffusion is slower, the difference in growth speed along more compact and less compact directions becomes more pronounced and star shaped domains are favoured, as can be seen in Figure 23. At higher temperature, growth becomes faster in all directions and the domains are hexagonal (Figure 22).

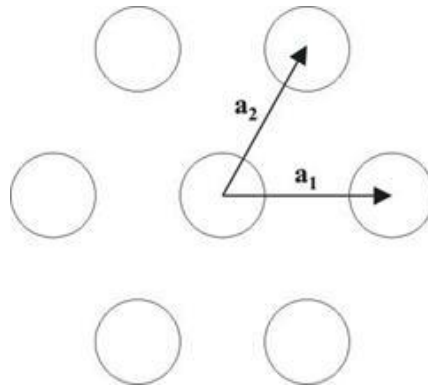


Figure 40 – Hexagonal Lattice.

An alternative mechanism to the pure nucleation-and-growth is a 2D Ostwald ripening process ^[20]. This mechanism is driven by the minimization of the phase boundary area and consists on the dissolution of the smaller domains in favour of the growth of the larger. This effect may be the reason for the large differences in domain size found in 18F films at high and low temperatures. At low temperature the size of domains is fairly constant. At high temperature the film is composed by a large number of small clusters and few large domains. Since mobility is larger at higher temperatures, the 2D Ostwald ripening process may be more pronounced. These evidences suggest that at the beginning the mechanism of crystallization may be controlled by typical 2D nucleation and growth and for longer times may be controlled by 2D Ostwald ripening process.

4. Conclusions

The surface tension of pure TFE was measured as a function of temperature (from 266.15K to 308.15K).

The surface tension of mixtures of TFE with ethanol, 1-propanol, 1-butanol and tert-butanol was measured at 293.15K. All mixtures display minima. The excess molar volume of mixtures of TFE and ethanol, 1-propanol, 1-butanol and tert-butanol was also measured at 293.15K. The excess molar volumes are all positive increasing with the chain length of hydrocarbon alcohol.

The mixtures display a very complex behaviour when compared with mixtures of hydrogenated alcohols and mixtures of alkanes and perfluoroalkanes, showing signs of high cohesion in the bulk and low cohesive forces at the surface.

Langmuir films of 18H, 14F, 18F and their mixtures were prepared on a Langmuir trough at several temperatures and transferred to the surface of silicon wafers. The Langmuir-Blodgett films were analysed by AFM.

Langmuir-Blodgett films of pure 18F display starry-hexagonal domains that form spontaneously at room temperature and low surface density. The domains are compatible with 2D crystals and seem to melt at higher temperature forming circular domains.

Langmuir-Blodgett films of pure 14F at room temperature display a “lacy” pattern that seem to crystalize at lower temperature forming starry-hexagonal domains.

Langmuir-Blodgett films of a mixture of 14F and 18F display a combination of the “lacy” patterns and hexagonal domains characteristic of the pure alcohols.

Langmuir-Blodgett films of a mixture of 18H and 18F display a combination of circular and hexagonal domains characteristic of the pure alcohols suggesting that the two alcohols phase separate in 2D.

Molecular dynamics simulations of the pure 18F Langmuir films seems to confirm the tendency of fluorinated species to spontaneously crystalize at the surface of water, as opposed to hydrogenated species that form liquid-like domains.

Molecular dynamics simulations of a mixture of 18H and 18F indicates that the fluorinated molecules are able to accommodate the hydrogenated molecules and partially maintain the ordered structure of the pure fluorinated film. The simulation results showed no evidence of phase separation within the time scale of the simulation.

5. Future Work

Some features of this work must be developed even further in order to have a more complete understanding of the factors influencing the phenomena of phase separation of fluorinated and hydrogenated alcohols mixtures and surface crystallization of fluorinated alcohols mixtures. As future work it is proposed to:

- Study of the surface tension of binary mixtures increasing the fluorocarbon alcohol chain.
- Study the influence of temperature and time in the Langmuir Films of 18F, in order to increase the control over the size and shape of the domains.
- Study of Langmuir films of pure hydrogenated alcohols with longer chains, in order to find the influence of the alkyl-alkyl forces in the alcohols.
- Study of the internal structure of the hexagonal shapes using x-Ray techniques.
- Study of the influence of system size in Molecular Dynamics Simulations.

6. Bibliography

¹ Schreiber, F. Structure and growth of self-assembling monolayers. *Progress in Surface Science*, **2000**, 65, 151-256

² Krafft, M.P. Fluorocarbons and fluorinated amphiphiles in drug delivery and biomedical, *Adv. Drug Deliv. Rev.* **2001**, 47, 209–228.

³ May, G. Fluid solutions, *Chem. Br.* **1997**, 33, 34–36.

⁴ Gross, U.; Papke, G.; Rudiger, S. Fluorocarbons as blood substitutes—critical solution temperatures of some perfluorocarbons and their mixtures, *J. Fluorine Chem.* **1993**, 61, 11–16.

⁵ Simons, J.H.; Dunlap, R.D. *J. Chem. Phys.* **1950**, 18, 335–346.

⁶ Rowlinson, J.S.; Swinton, F.L. Liquids and Liquid Mixtures, third ed., Butterworth Scientific, London, **1982**.

⁷ Siebert, E.M.D.; Knobler, C.M.; Interaction virial coefficients in hydrocarbon–fluorocarbon mixtures, *J. Phys. Chem.* **1971**, 75, 3863–3870.

⁸ Brode, S.; McDonald, I.R. Excess thermodynamic properties of liquid-mixtures of methane and perfluoromethane, *Mol. Phys.* **1988**, 65, 1007–1012.

⁹ Schoen, M.; Hoheisel, C. Liquid Ch₄, liquid Cf₄ and the partially miscible liquid-mixture Ch₄/Cf₄—a molecular-dynamics study based on both a spherically symmetrical and a 4-center Lennard-Jones potential model, *Mol. Phys.* **1986**, 58, 699–709.

¹⁰ Archer, A.L.; Amos, M.D.; Jackson, G.; McLure, I.A. The theoretical prediction of the critical points of alkanes, perfluoroalkanes, and their mixtures using bonded hard-sphere (BHS) theory, *Int. J. Thermophys.* **1996**, 17, 201–211.

¹¹ Cui, S.T.; Cochran, H.D.; Cummings, P.T. Vapor–liquid phase coexistence of alkane, carbon dioxide and perfluoroalkane carbon dioxide mixtures, *J. Phys. Chem. B.* **1999**, 103, 4485–4491.

¹² McCabe, C.; Galindo, A.; Gil-Villegas, A.; Jackson, G. Predicting the high-pressure phase equilibria of binary mixtures of perfluoroalkanes plus n-alkanes using the SAFT–VR approach, *J. Phys. Chem. B.* **1998**, 102, 8060–8069.

¹³ Duce, C.; Tine, M.R.; Lepori, L.; Matteoli, E. VLE and LLE of perfluoroalkanes + alkane mixtures, *Fluid Phase Equilib.* **2002**, 199.

¹⁴ Schneider, G.M. High-pressure phase equilibria and spectroscopic investigations up to 200MPa on fluid mixtures containing fluorinated compounds: a review, *Fluid Phase Equilib.* **2002**, 199, 307–317.

¹⁵ Song, W.; Rosky, P.J.; Maroncelli, M.; Modeling alkane–perfluoroalkanes interactions using all-atom potentials: failure of the usual combining rules, *J. Chem. Phys.* **2003**, 119, 9145–9162.

¹⁶ Duarte, P.; Silva, M.; Rodrigues, D.; Morgado, P.; Martins, L. F. G.; Filipe, E. J. M. Liquid Mixtures Involving Hydrogenated and Fluorinated Chains: (p, ρ, T, x) Surface of (Ethanol + 2,2,2-Trifluoroethanol), Experimental and Simulation. *J. Phys. Chem. B* **2013**, 117, 9709-9717.

¹⁷ McLure, I. A.; Edmonds, B.; Lal, M. Extremes in Surface-Tension of Fluorocarbon + Hydrocarbon Mixtures. *Nature-Physical Science* **1973**, 241, 107, 71-71.

¹⁸ Handa, T.; Mukerjee, P. Surface Tensions of Nonideal Mixtures of Fluorocarbons and Hydrocarbon and Their Interfacial tensions against Water. *J. Phys. Chem.* **1981**, 85, 3916-3920.

-
- ¹⁹ Qaqish, S. E.; Paige M. F. Structural and Compositional Mapping of a Phase-Separated Langmuir-Blodgett Monolayer by Atomic Force Microscopy. *Langmuir* **2007**, *23*, 2582-2587.
- ²⁰ Qaqish, S. E.; Paige M. F. Characterization of domain growth kinetics in a mixed perfluorocarbon-hydrocarbon Langmuir-Blodgett monolayer. *Journal of Colloid and Interface Science* **2008**, *325*, 290-293.
- ²¹ Yuan, Y.; Lee, T. R. Contact Angle and Wetting Properties. *Springer series in Surface Sciences* **2013**, *51*, 3-34.
- ²² Kissa, E. *Fluorinated surfactants*; Surfactant Science Series, **1994**
- ²³ Gaines, G. *Insoluble Monolayers at Liquid-Gas Interfaces*; Interscience Publishers, **1966**.
- ²⁴ Israelachvili, J. *Intermolecular & Surfaces Forces*; second edition; Academic Press, **1991**.
- ²⁵ Adamson, A. W.; Gast, A. P. *Physical Chemistry of Surfaces*; sixth edition; Wiley-Interscience Publication, **1997**.
- ²⁶ Pockels, A. *Nature* **1891**, *43*, 437
- ²⁷ Frenkel, D; Smit, B. Understanding Molecular Simulation. *Academic Press*, **2002**.
- ²⁸ Allen, M.P.; Tildesley, D.J. Computer Simulation of Liquids. *Oxford University Press*, **1991**
- ²⁹ Smith, W.; Forester, T. R.; Todorov, I. T. The DL_POLY Classic User Manual, version 1.9, April 2012, STFC Daresbury Laboratory.
- ³⁰ Río, O. I.; Neumann, A. W. Axisymmetric Drop Shape Analysis: Computational Methods for the Measurement of Interfacial Properties from the Shape and dimension of Pendant and Sessile Drops. *Journal of Colloid and Interface Science* **1997**, *196*, 136-147.
- ³¹ Hoorfar, M.; Neumann, A. W. *Adv. Colloid Interface Sci.* **2006**, *121*, 25
- ³² Hermansson, K.; Lindberg, U.; Hok, B.; Palmkog, G. Wetting Properties of Silicon Surfaces. *Solid-State Sensors and Actuators Conference*, **1991**, 193-196
- ³³ I. Horcas *et al.* *Rev. Sci. Instrum.* **2007**, *78*, 013705
- ³⁴ Jorgensen, W. L.; Maxwell, D. S.; Tirado-Rives, J. Development and Testing of the OPLS All-Atom Force Field on Conformational Energetics and Properties of Organics Liquids. *J. Am. Chem. Soc.* **1996**, *118*, 11225-11236
- ³⁵ Berendsen, H. J. C.; Grigera, J. R.; Straatsma, T. P. The Missing Term in Effective Pair Potentials. *J. Phys. Chem.* **1987**, *91*, 6269–6271.
- ³⁶ Humphrey, W.; Dalke, A.; Schulten, K. VMD - Visual Molecular Dynamics. *J. Molec. Graphics.* **1996**, *14*, 33-38.
- ³⁷ Kim, K. S.; Lee, H. *J. Chem. Eng. Data* **2002**, *47*, 216
- ³⁸ The Landolt-Bornstein Database, Surface Tension of Pure Liquids and Binary Liquid Mixtures – Supplement to IV/16. *Springer-Verlag* **2008**, 24.
- ³⁹ Jasper, J. J. The Surface Tension of Pure Liquid Compounds. *J. Phys. Chem.* **1972**, *1*, 4, 841-1007.
- ⁴⁰ Sassi, M; Atik, Z. Excess Molar Volumes of Binary Mixtures of 2,2,2-Trifluoroethanol with water, or Acetone, or 1,4-Difluorobenzene, or 4-Fluorotoluene, or alpha, Alpha, Alpha Trifluorotoluene or 1-

Alcohols at a Temperature of 298.15K and Pressure of 101 kPa. *J. Chem. Thermodyn.* **2003**, 35, 1161-1169

⁴¹ Atik, Z. Densities and Excess Molar Volumes of Binary and Ternary Mixtures of Aqueous Solutions of 2,2,2-Trifluoroethanol with Acetone and Alcohols at the Temperature of 298.15K and Pressure of 101kPa, *Journal of Solution Chemistry*, **2004**, 33, 11, 1447-1466

⁴² Minamihonoki, T.; Ogawa, H.; Nomura, H.; Murakami, S. Thermodynamic Properties of Binary Mixtures of 2,2,2-Trifluoroethanol with Water or Alkanol at T=298.15K. *Thermochim. Acta* **2007**, 459, 80-86

⁴³ Smith, L. S.; Tucker, E. E.; Christian, S. D. Vapor-Density and Liquid-Vapor Equilibrium Data for Binary Mixtures of 2,2,2-Trifluoroethanol with Water, Methanol, Ethanol, and 2-Butanol. *J. Phys. Chem.* **1981**, 85, 1120-1126

⁴⁴ Mejia, A.; Cartes, M.; Segura, H. Interfacial tensions of binary mixtures of ethanol with octane, decane, dodecane and tetradecane. *J. Chem. Thermodynamics*, **2011**, 43, 1395-1400.

⁴⁵ Bowers, I.; Mclure, I. A.; Whitfield, R. Surface Composition Studies on (n-Hexane + Perfluoro-n-hexane) by Specular Neutron Reflection. *Langmuir* **1997**, 13, 2167-2170.

⁴⁶ Gamboa, A. L. S. Ordering in Langmuir and Langmuir-Blodgett Films: effect of the presence of fluorocarbon and hydrocarbon chains. *Instituto Superior Técnico* **2006**